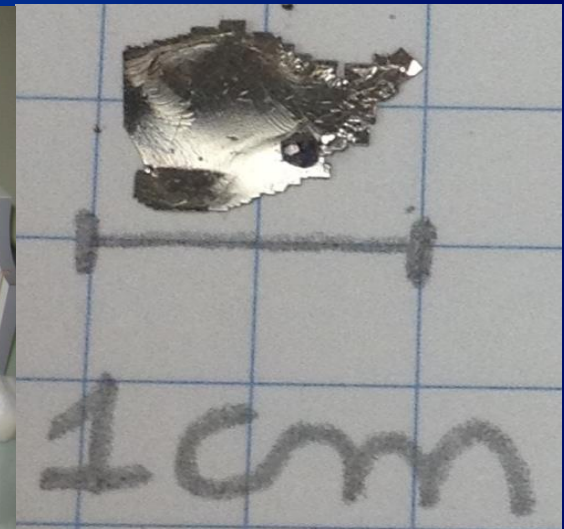
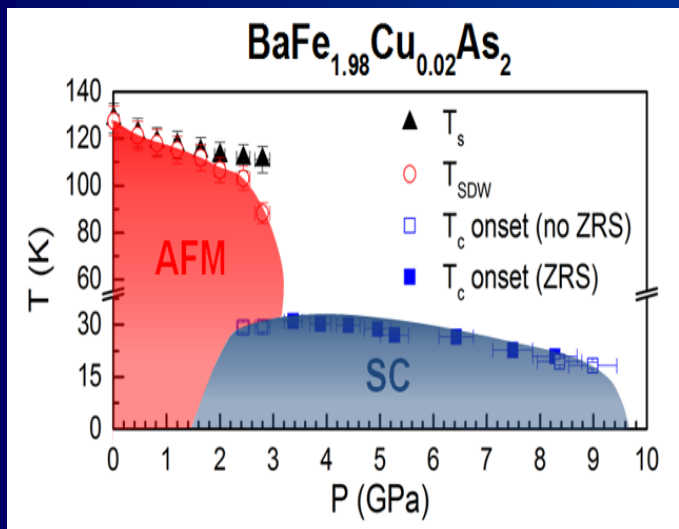


Workshop on Next Generation Quantum Materials

Combined external pressure and chemical substitution studies on $\text{BaFe}_{1.98}\text{Cu}_{0.02}\text{As}_2$ single crystals



Outline

I. Motivation – Fe-based SC

II. In-flux crystals growth

III. The role of local distortions in the Fe-site

V. Actual doping x orbital differentiation of the Fe 3d bands?

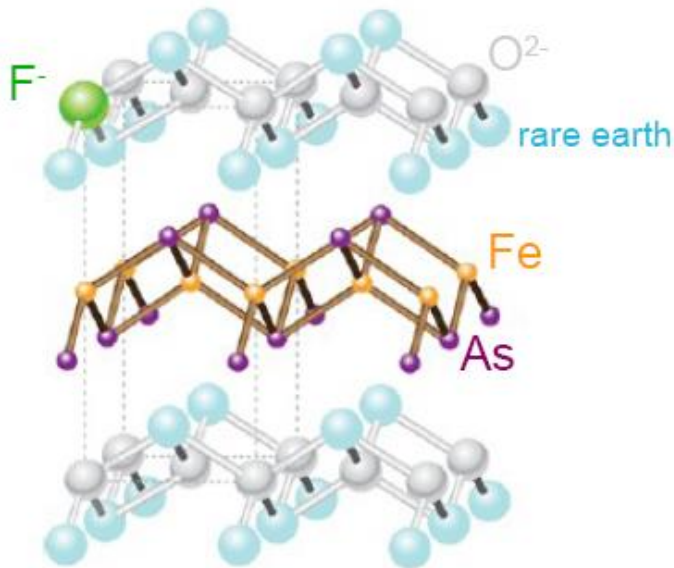
VI. Combined pressure and chemical substitution experiments

VII. The particular case of Cu-substitution in BaFe_2As_2

VIII. Final Remarks

Motivation

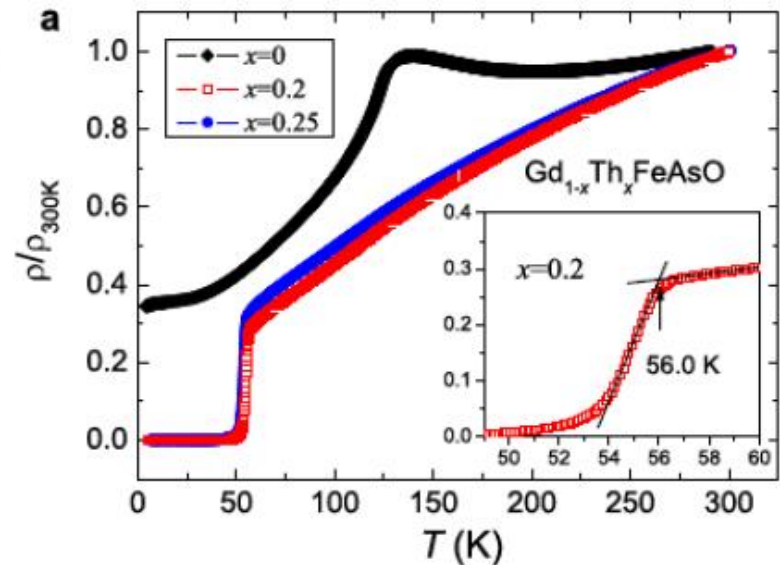
- Initial Discovery: $\text{LaFeAsO}_{1-x}\text{F}_x$ (Kamihara et al., 2008, $T_c = 26 \text{ K}$) – T_c can get as high as $\sim 56 \text{ K}$ for $R = \text{Gd}$.



Initial discovery: $T_c = 28 \text{ K}$ in

F-doped LaOFeAs

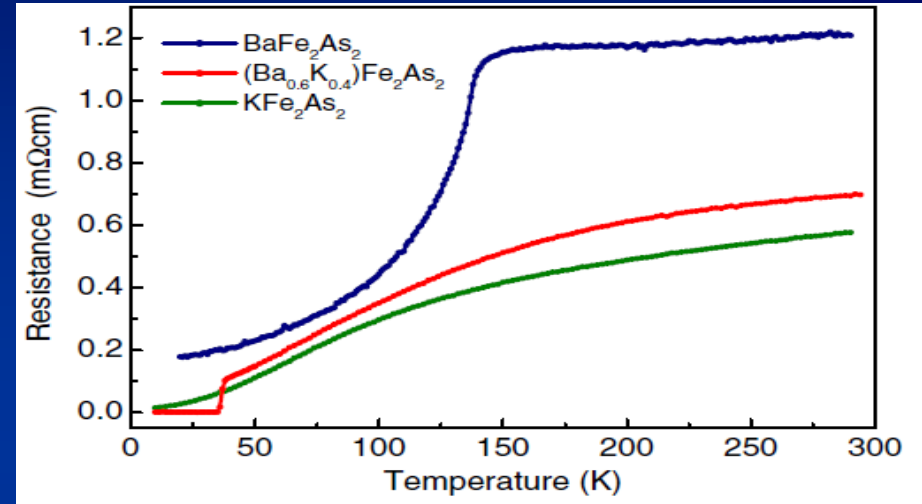
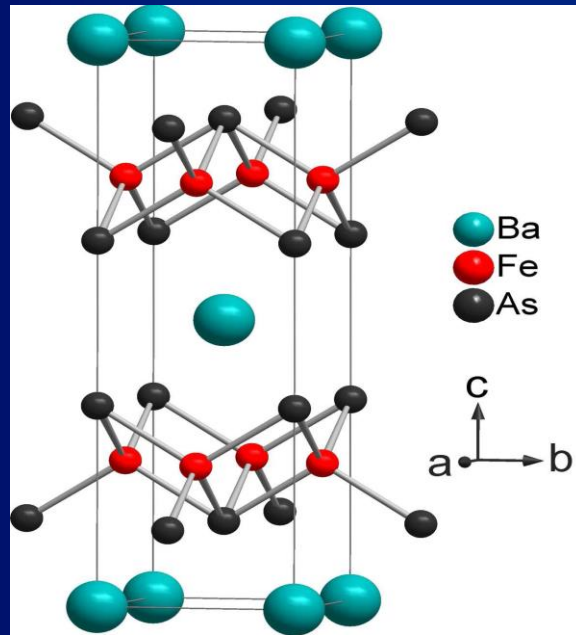
Y. Kamihara, T. Watanabe, M. Hirano, and H. Hosono, *J. Am. Chem. Soc.* **130**, 3296 (2008).



C. Wang et al., *Europhys. Lett.* **83**, 67006 (2008).

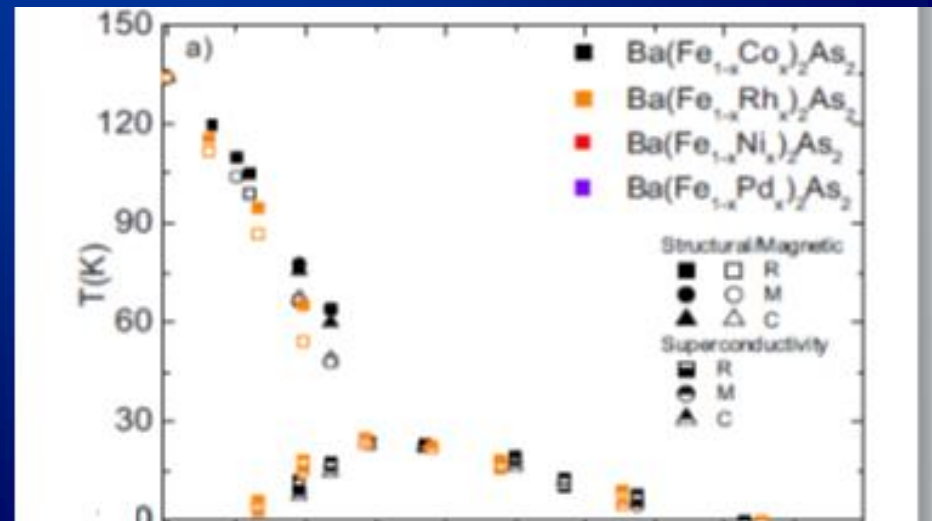
Motivation

Discovery of Oxygen free intermetallic “relatives”: $\text{Ba}_{1-x}\text{K}_x\text{Fe}_2\text{As}_2$ (Rotter et al., 2008, $T_c \sim 40$ K).



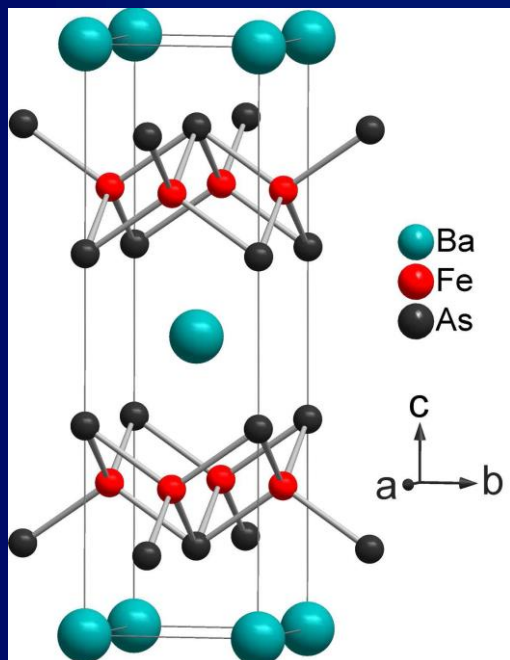
M. Rotter et al., Phys. Rev. Lett. **101**, 107006 (2008)

Two classes of FeAs-based materials (oxides and intermetallic compounds) with comparable T_c s and phase diagrams!!

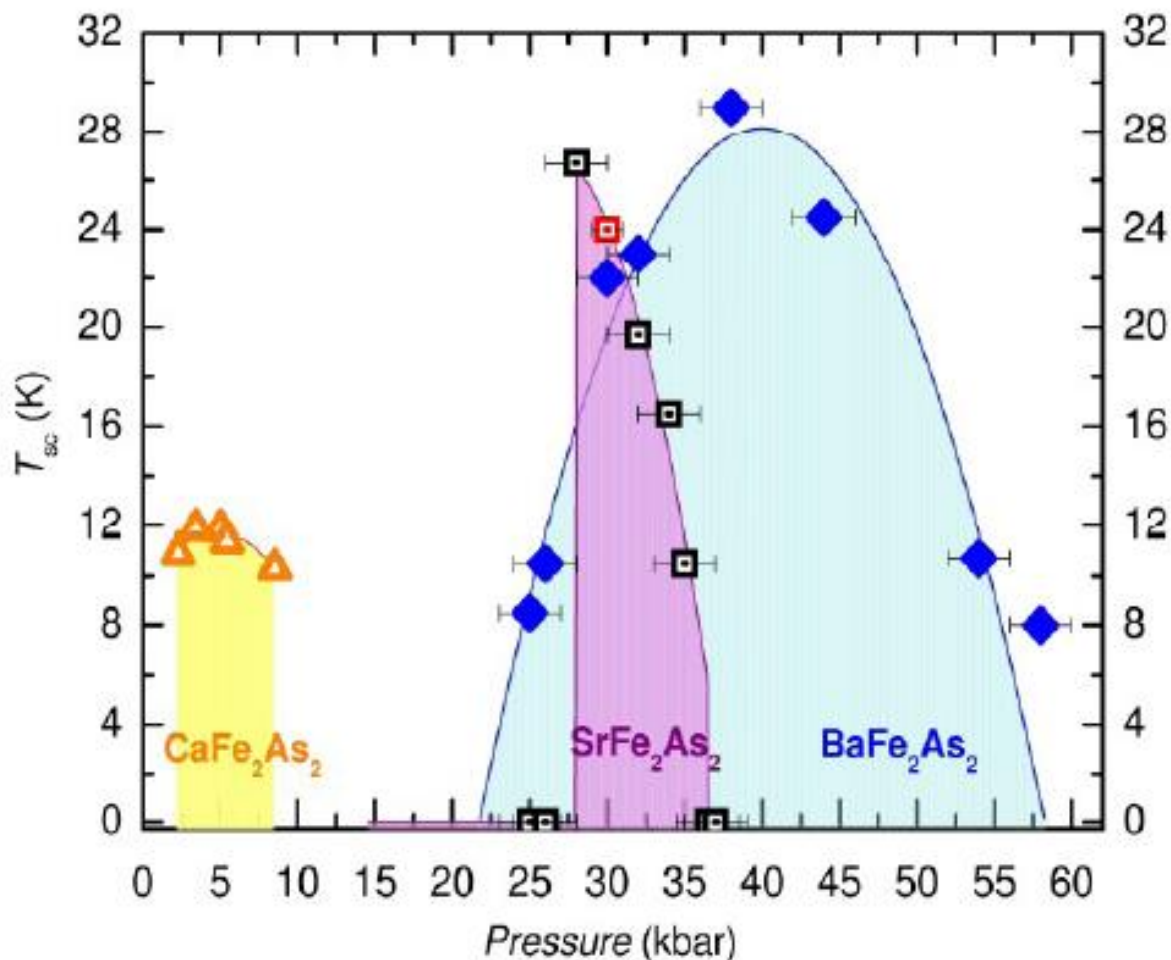


N. Ni et al., Phys. Rev. B **80**, 024511 (2009)

Pressure induced SC – similar to HFS

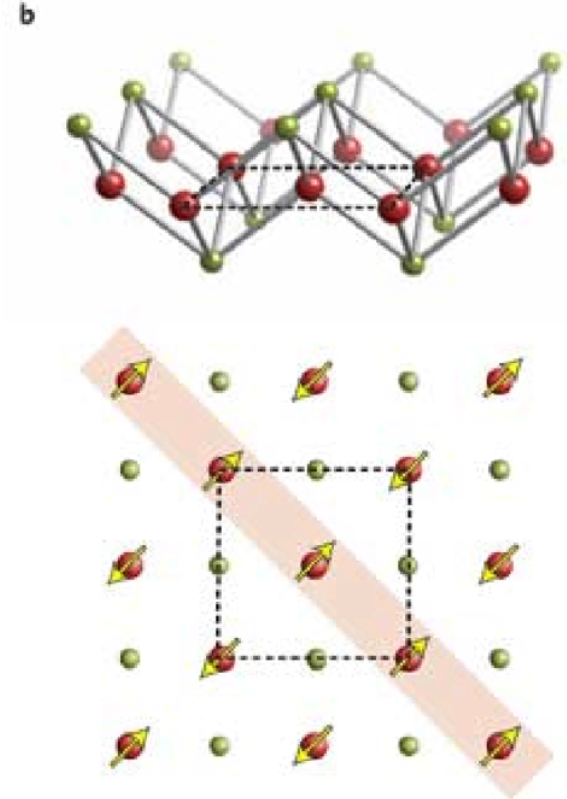
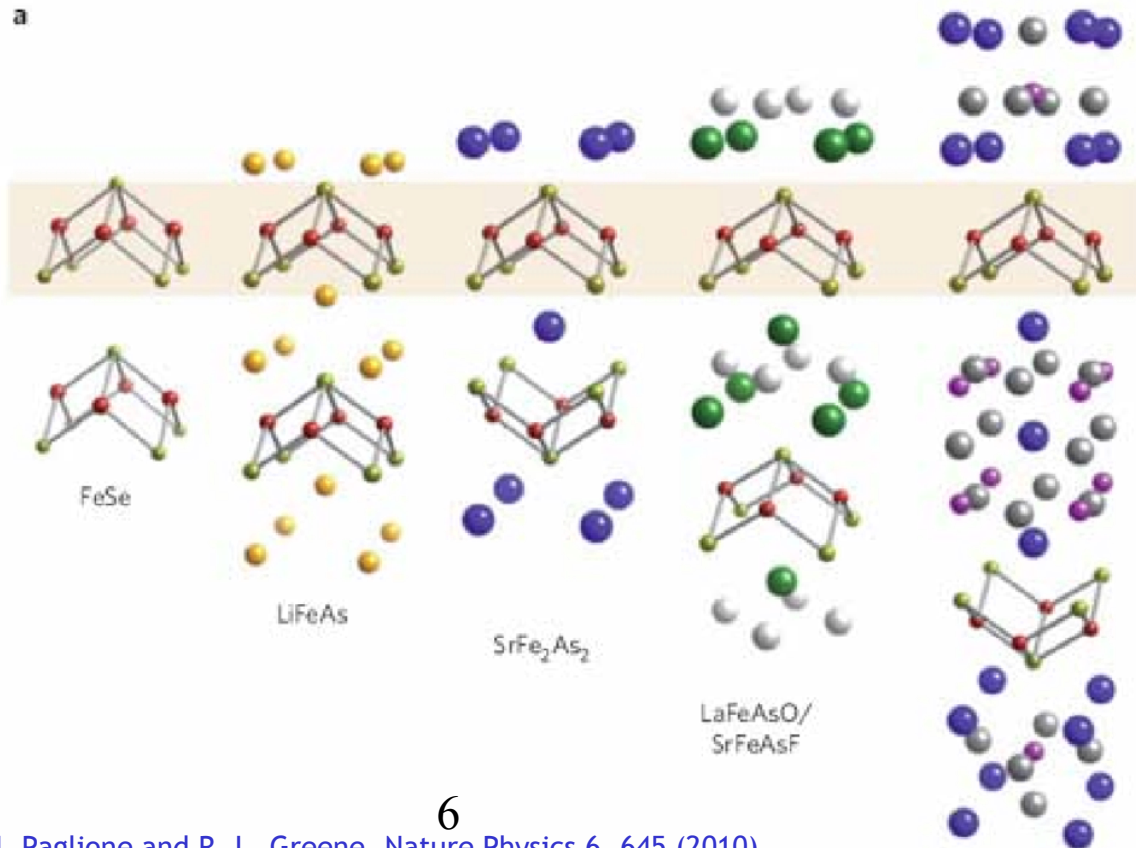


- M. S. Torikachvili, S.L. Bud'ko, N. Ni, and P.C. Canfield, Phys. Rev. Lett. **101**, 057006 (2008);
• ibidem Phys. Rev. B **78**, 104527 (2008).
- P. Alireza *et al.*, J. Phys.: Condens. Matter **21**, 012208 (2009).
- T. Park *et al.*, J. Phys.: Condens. Matter **20**, 322204 (2008).
- H. Fukasawa *et al.*, condmat/0808.0718.
- A. Mani *et al.*, cond-mat/0903.4236.
- E. Colombier, S.L. Bud'ko, N. Ni, and P.C. Canfield, condmat/0904.4488.



Fe-based superconductors

- ❖ Common Structural parameter: $\text{Fe}(\text{As},\text{Se})_4$ tetrahedral
- ❖ Common Electronic parameter: SDW magnetic instability



Open Questions!

- 1) What is main microscopic tuning parameter responsible for driving SDW to SC ?
- 2) Are the structural and SDW phase transitions first or second order?
- 3) Do these two transitions happen simultaneously/independently? Do they have direct influence on the emergence of the SC phase?
- 4) What are the universal emergent phenomena in the Fe-based SC regarding the pairing mechanism and the SC gap symmetry?
- 5) What is the real potential for application of the existing Fe-based superconductors?

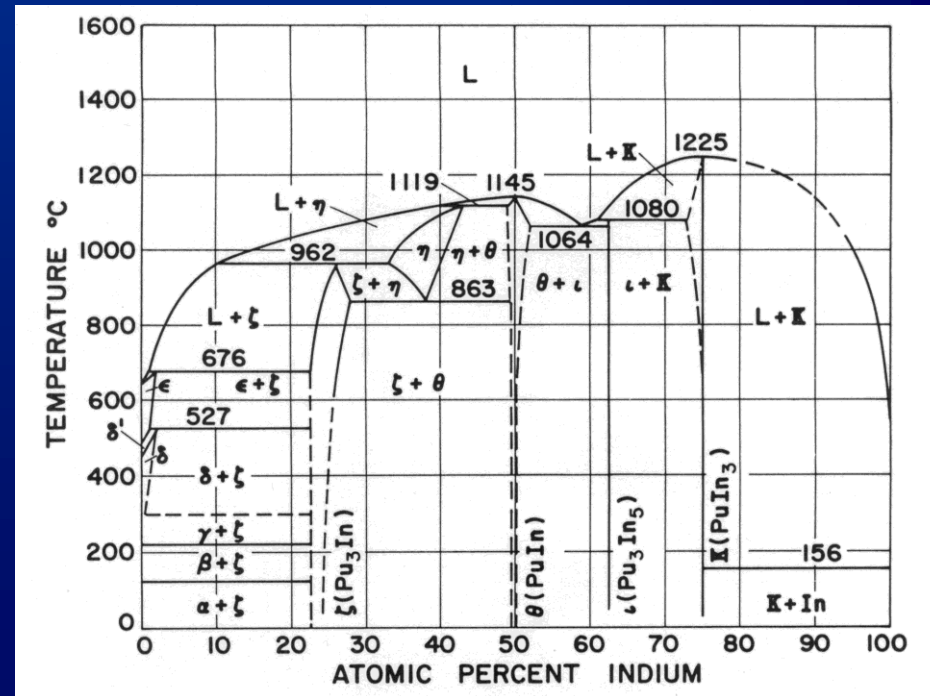
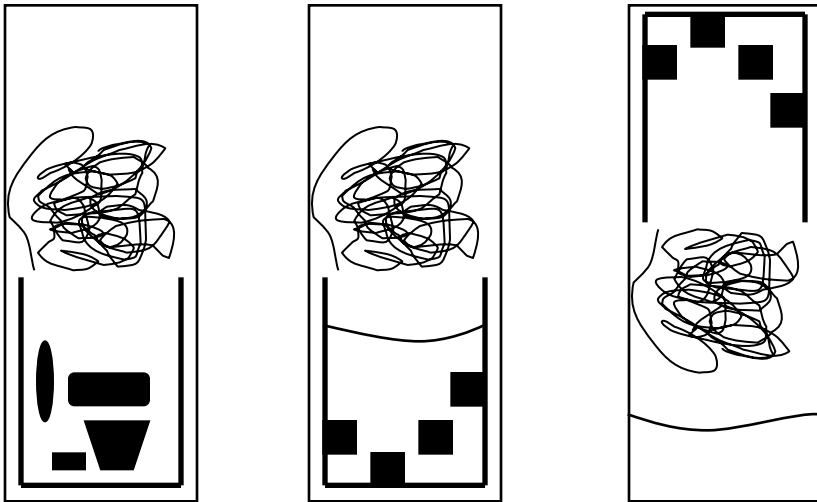
Flux Growth - Introduction

Growth of single crystals from low-melting solvents

- Simple hardware/inert atmosphere
- Low temperature / short time process
- Self-cleaning / well-faceted morphologies

Fisk & Remeika (1989)

Canfield & Fisk (1992)



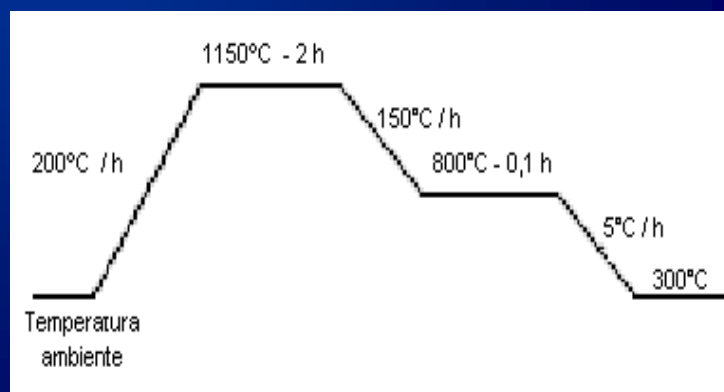
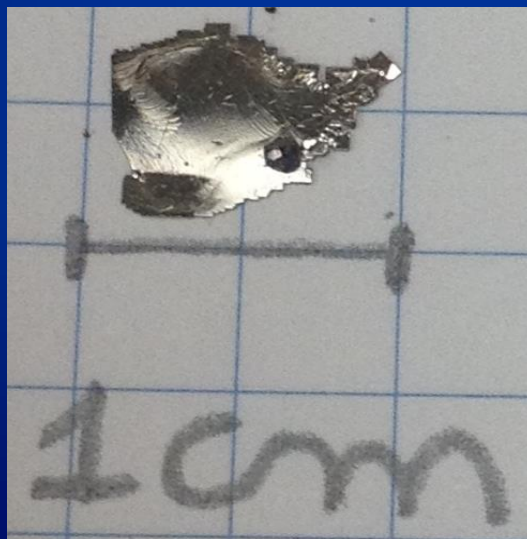
Metallic Flux Growth



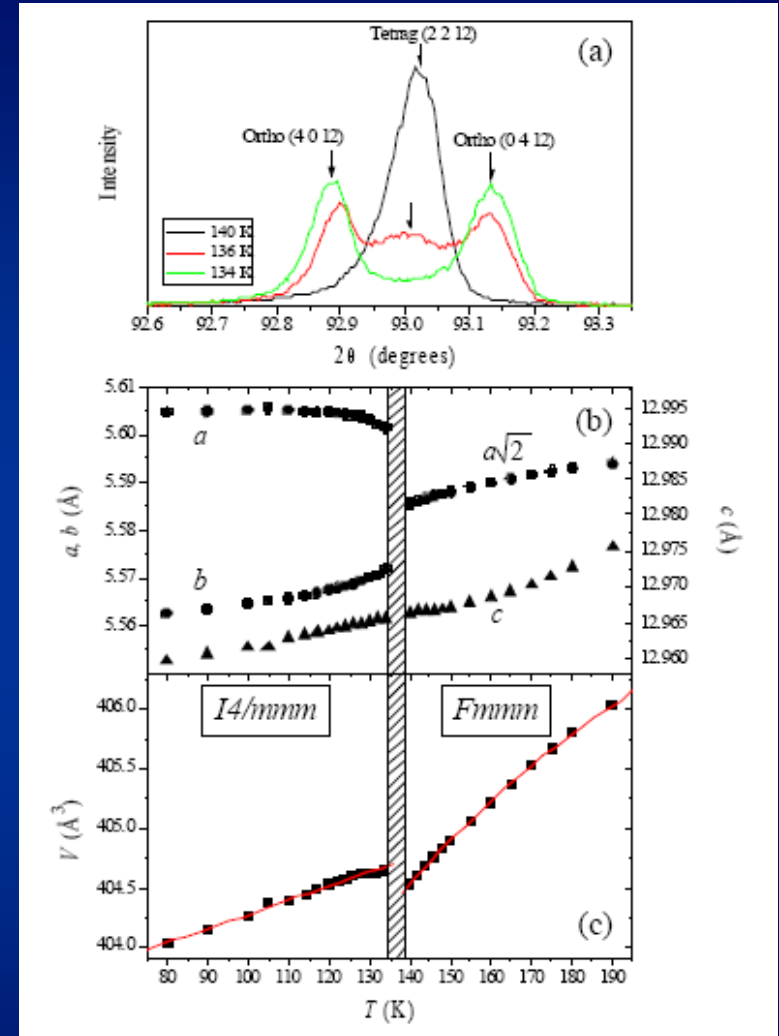
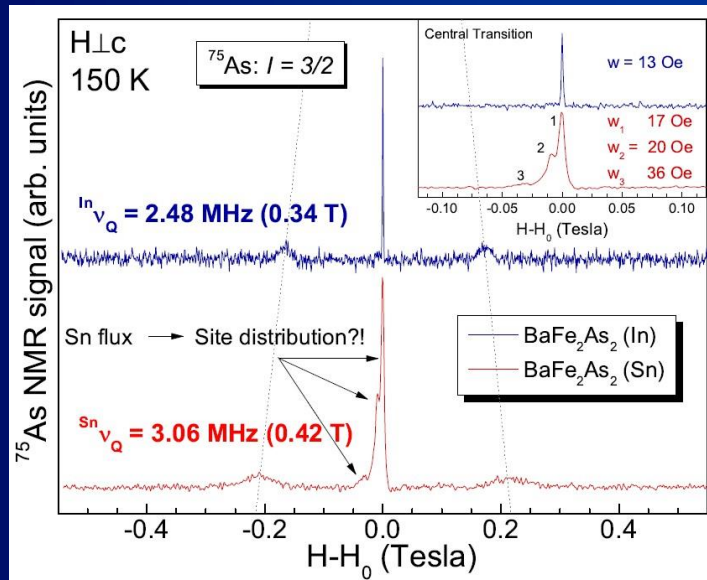
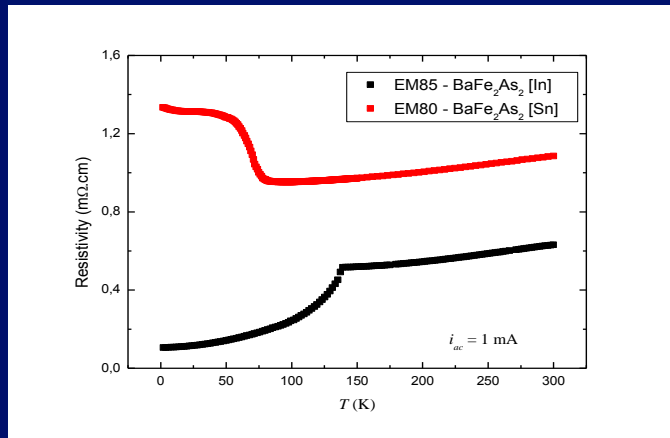
Metallic Flux Growth



In-flux samples growth at GPOMS - Campinas



Comparison BaFe_2As_2 : In- e Sn



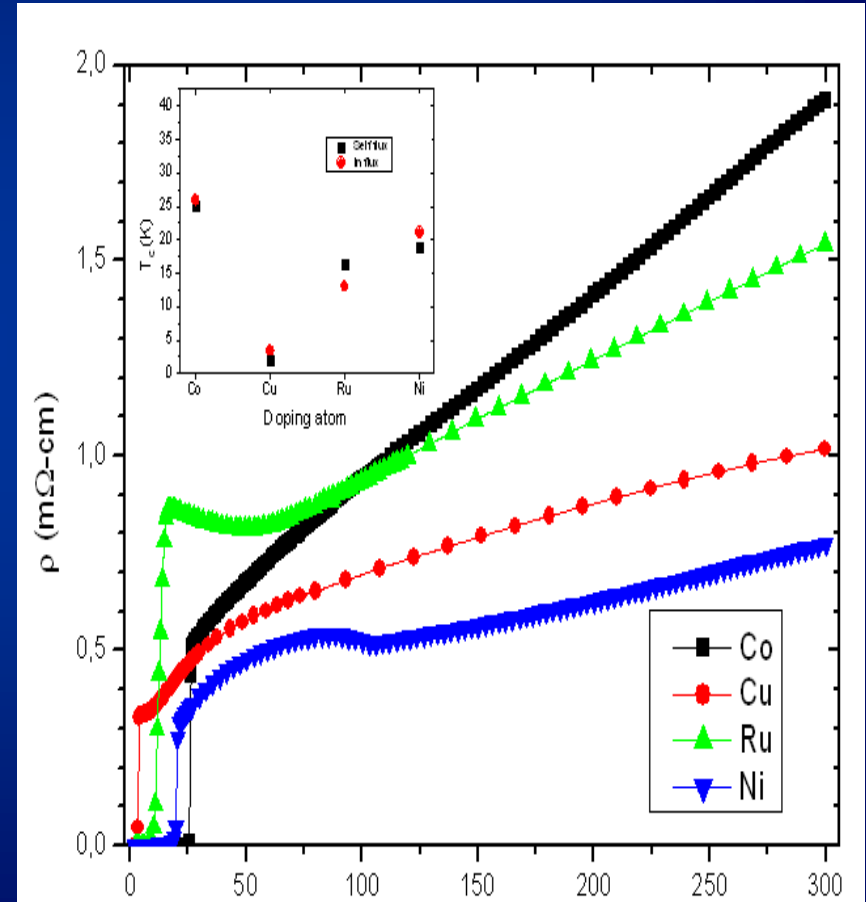
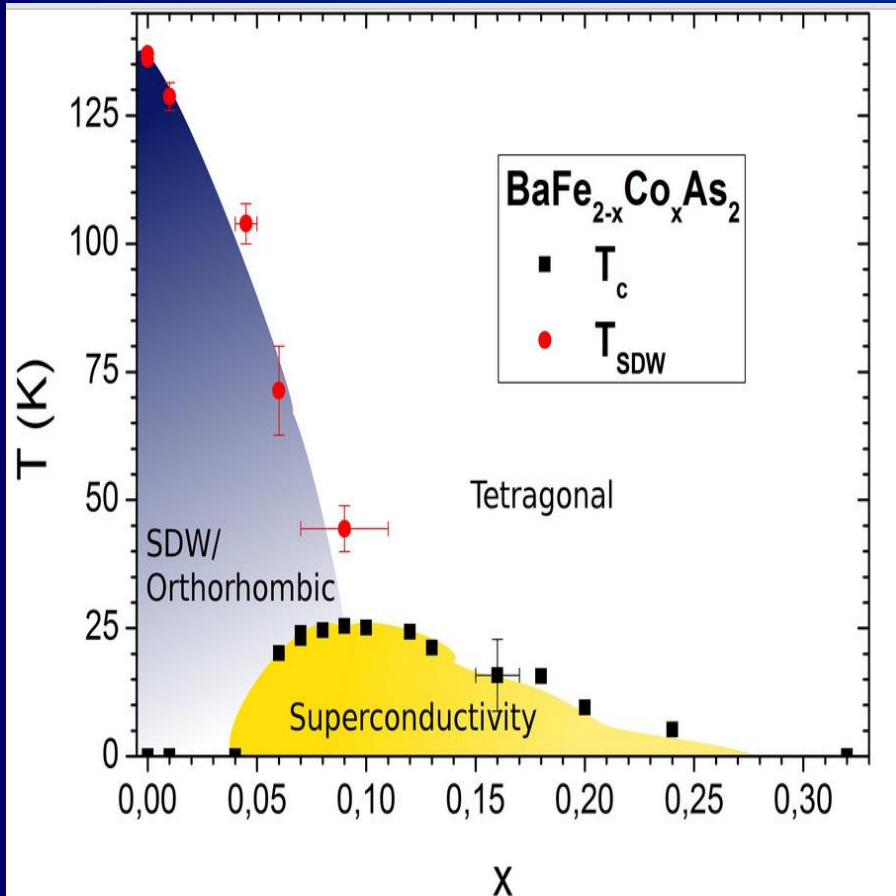
R. R. Urbano... P. G. Pagliuso *et al*, *Phys. Rev. Lett.* **105** 107001 (2010).

T. M. Garitezi... P. G. Pagliuso *et al* 2013 *Braz. J. Phys.* **43**, 223-229 (2013).

In-flux grown samples are free of In – inclusion

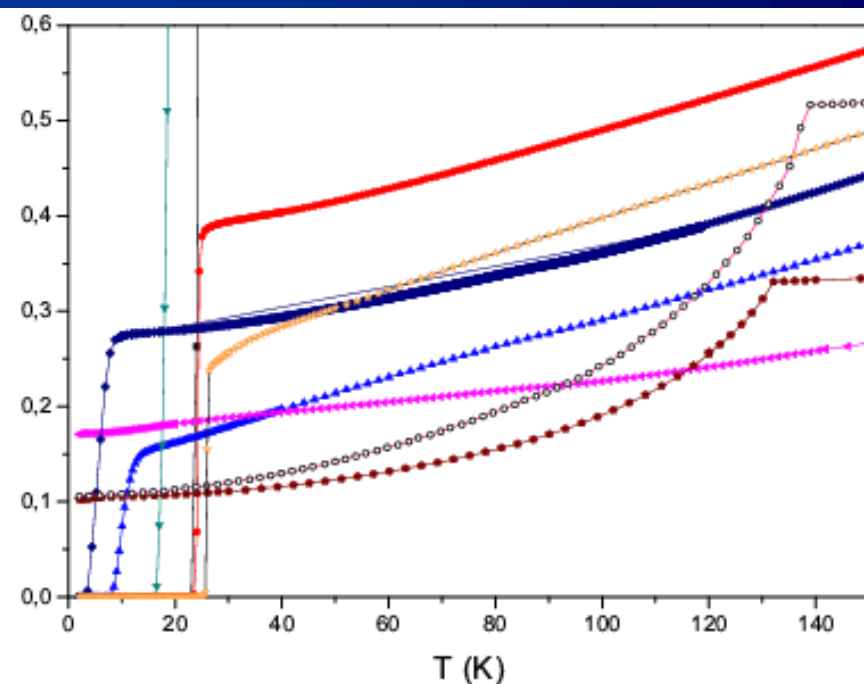
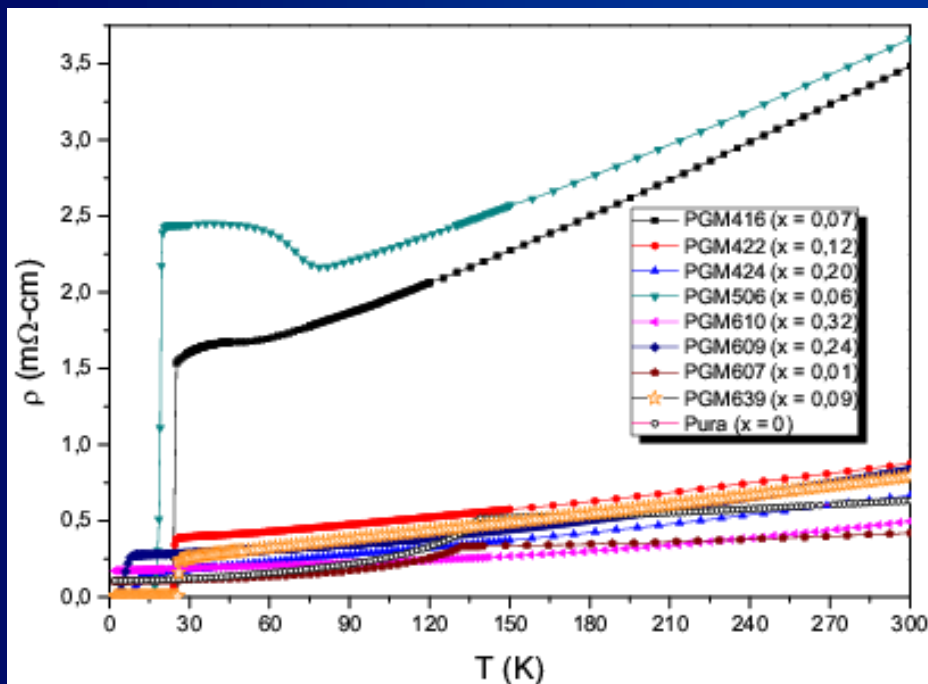
Results – In flux grown samples

- Phase Diagram and T_c s for OPD samples



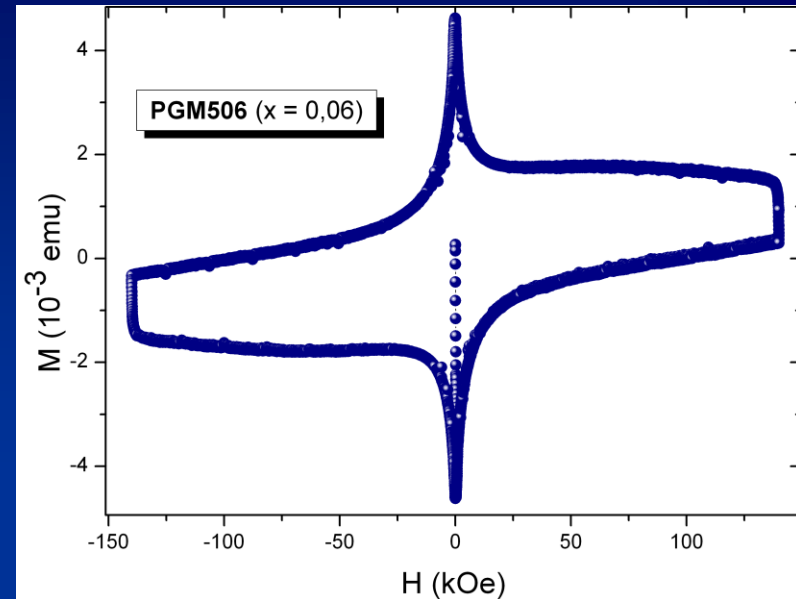
Results – In-flux grown samples

- Resistividade DC
 - Doping evolution
 - Residual Resistivity : $0.1 \leq \rho \leq 0.7 \text{ m}\Omega\text{-cm}$, similar and/or smaller than self-flux samples (PRB **82**, 220504 e 064501 (2010)), but no need of As excess!



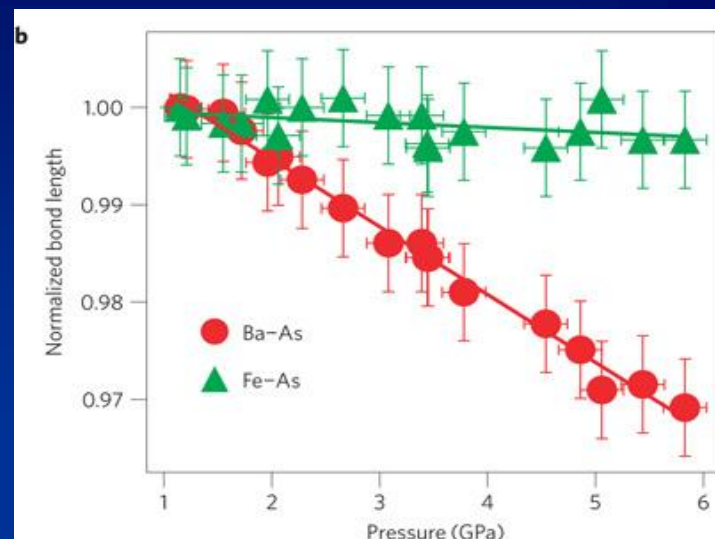
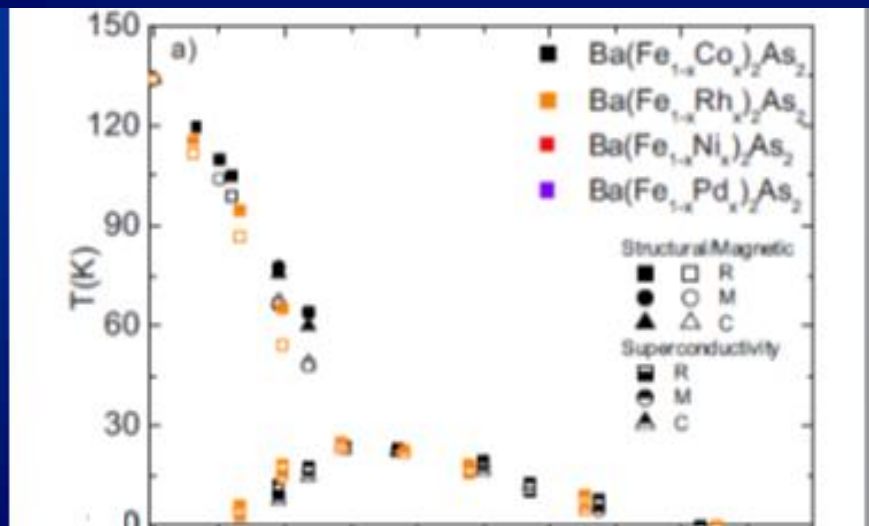
Results – In-flux grown samples

- J_c 's similar or smaller than self-flux samples ($J_c \sim 10^6$ A/cm²) (arXiv:0911.5582v1; PRB 80, 174517 (2009); Appl. Phys. Lett. 94, 062511 (2009); arXiv:1011.5721v1)
- High quality samples!



Samples	J_c (2 K, H = 0) (A/cm ²)	H_{c1} (Oe)	$\sim\lambda$ (nm)
PGM505 (x = 0,16)	$2,9 \cdot 10^6$	~ 7500	---
PGM506 (x = 0,06)	$7,5 \cdot 10^4 - 6,2 \cdot 10^5$	~ 240	165
PGM507 (x = 0,18)	$5,8 \cdot 10^3$	~ 360	---
PGM424 (x = 0,20)	---	~ 250	145
PGM416 (x = 0,07)	$1,1 \cdot 10^4$	~ 2000	48

Results – EXAFS – Decrease of d(Fe-As)



Kimber S.A.J. et al., Nat. Mat. 8, 471 (2009)

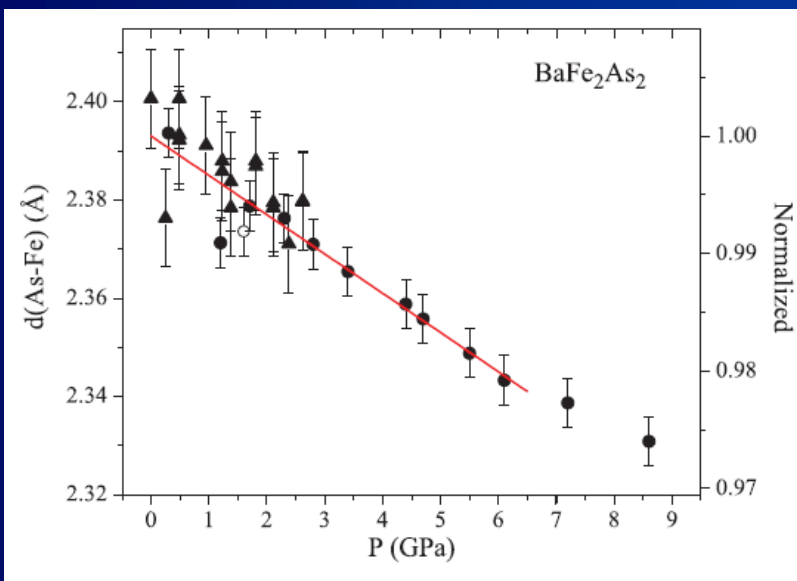
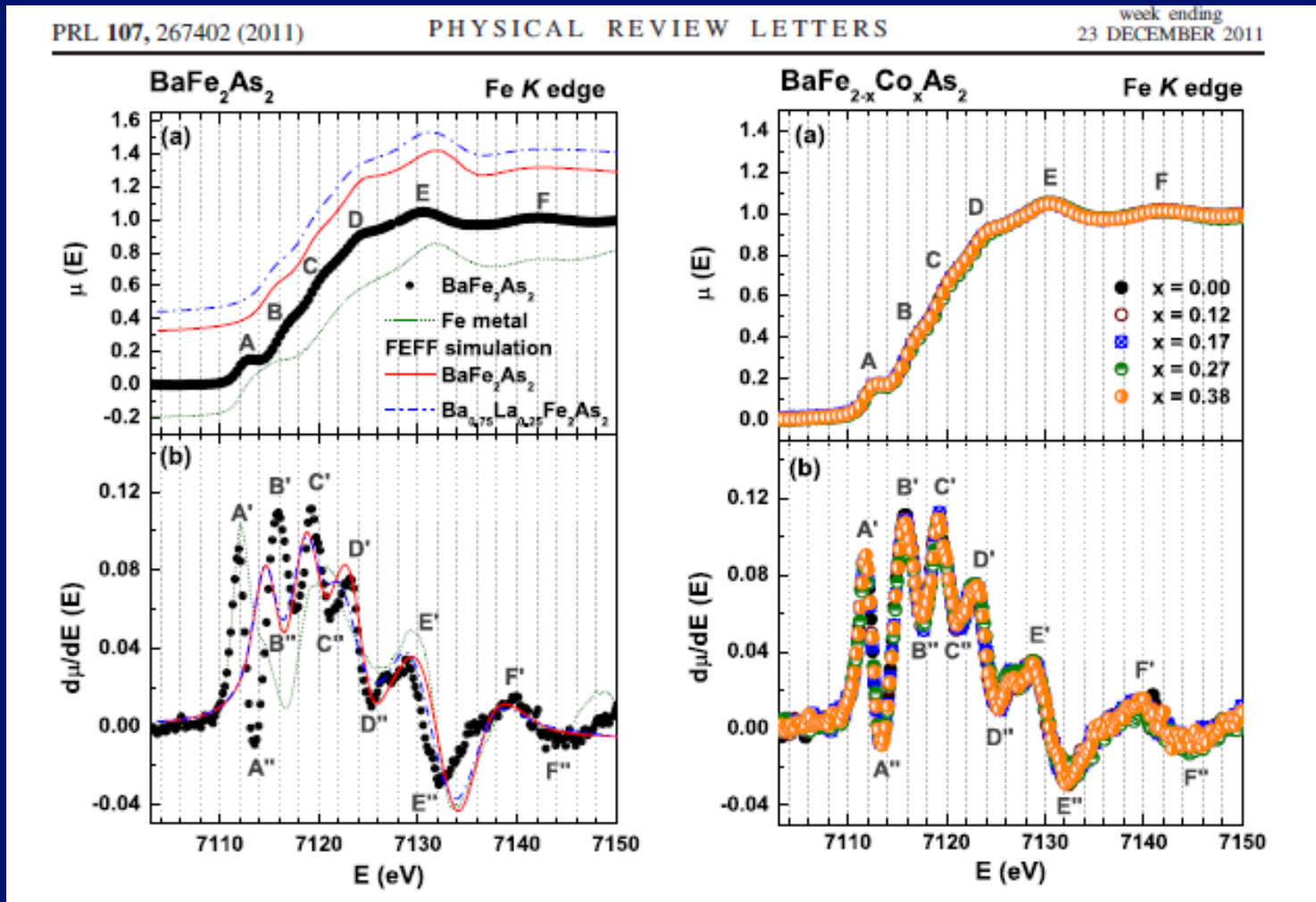


TABLE I. Refined As-*M* (*M* = Fe, Co) distances and Debye-Waller factors obtained from the fits of x-ray absorption fine structure data at the As *K* edge at ambient pressure. Errors given in parentheses are statistical only, and are defined as the standard deviation of the results obtained from repeated measurements under identical conditions.

	<i>T</i> = 2 K	<i>T</i> = 30 K	<i>T</i> = 298 K
BaFe₂As₂			
<i>d</i> (As-Fe) (Å)	2.3915(12)	2.3914(7)	2.3985(14)
σ^2 (Å ²)	0.00266(12)	0.00250 (7)	0.00465(11)
Ba[Fe_{0.937}Co_{0.063}]₂As₂			
<i>d</i> [As-(Fe,Co)] (Å)	2.3833(12)	2.3838(9)	2.3951(12)
σ^2 (Å ²)	0.00262(12)	0.00268(9)	0.00466(9)
Ba_{0.85}K_{0.15}Fe₂As₂			
<i>d</i> (As-Fe) (Å)	2.3865(15)	2.3900(12)	2.3955(9)
σ^2 (Å ²)	0.00242(15)	0.00248(12)	0.00466(7)

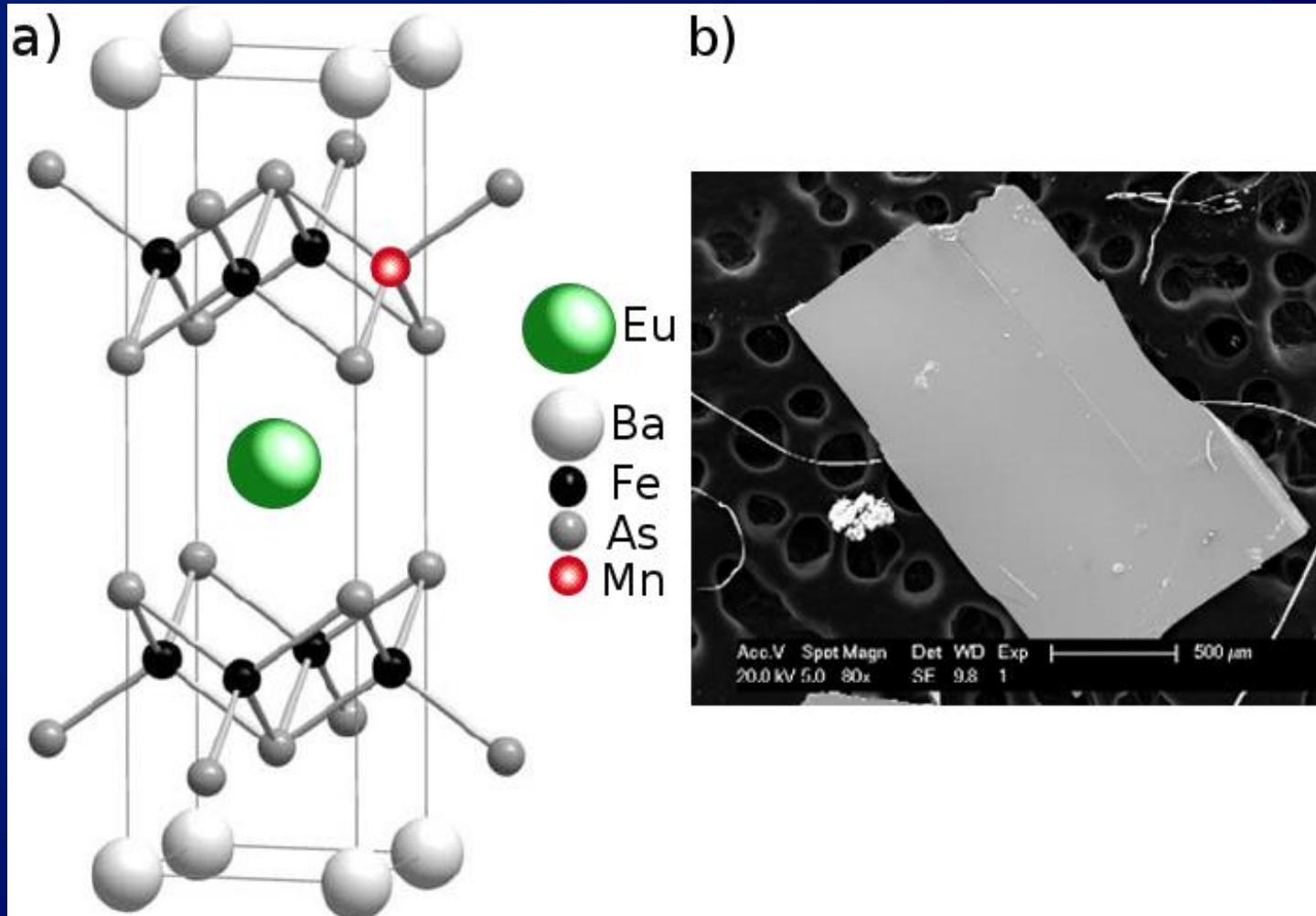
Results – XANES on In-flux grown samples



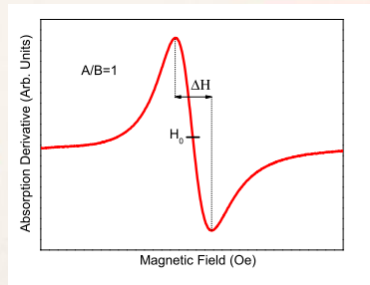
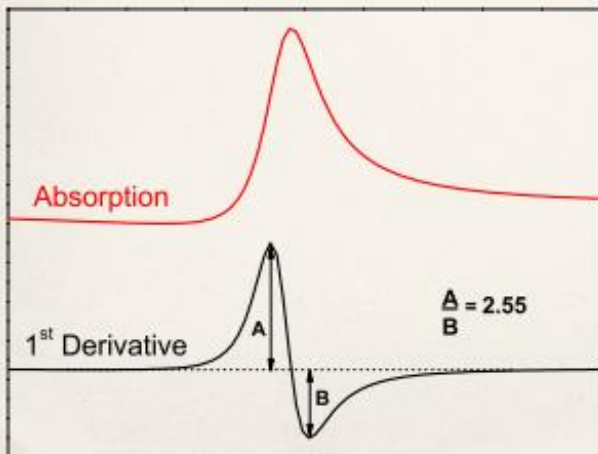
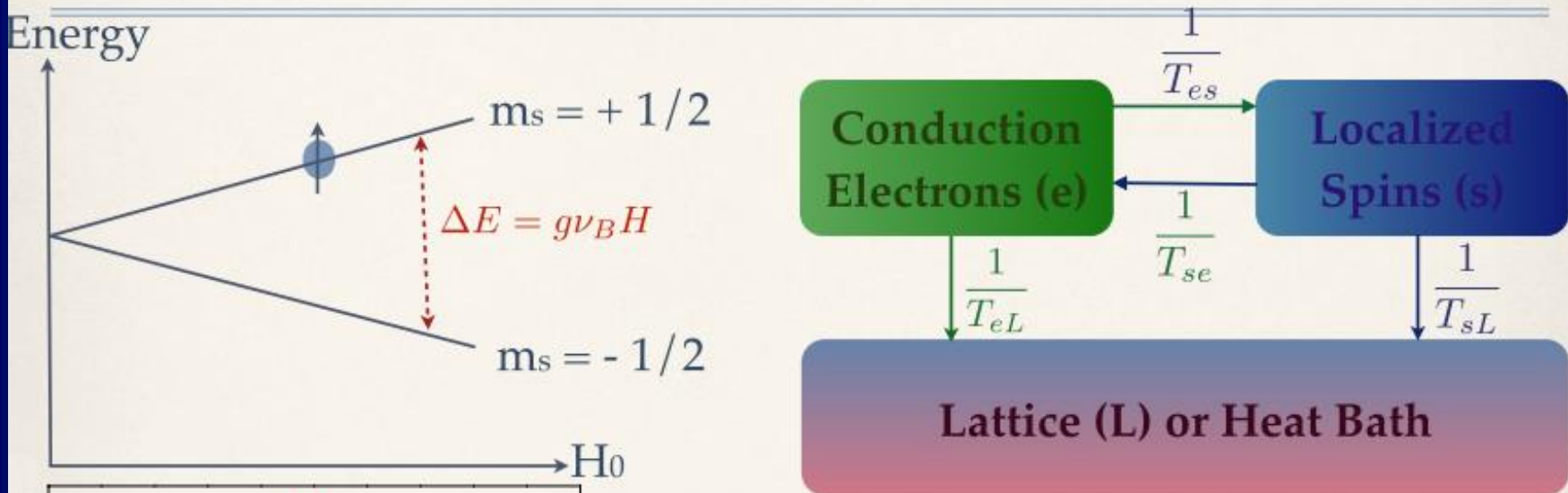
E. M. Bittar ... P.G. Pagliuso et al. PRL 107, 267402 (2011).

Fe K absorption edge is completely unaltered by Co-substitution!

Site specific ESR on Fe-based Intermetallic Compounds



Electron spin resonance (ESR): Relaxation Mechanism in Metals



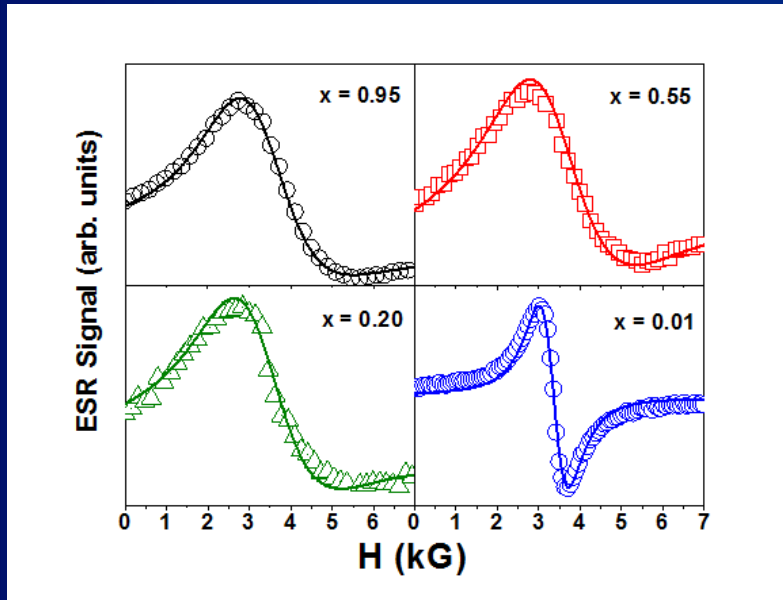
$H_0 \rightarrow$ g-value or IT
 $\Delta H \rightarrow$ relaxation and inhomogeneity

$$I \rightarrow \chi(T)$$

J. Korringa. Physica 16, 601 (1950).

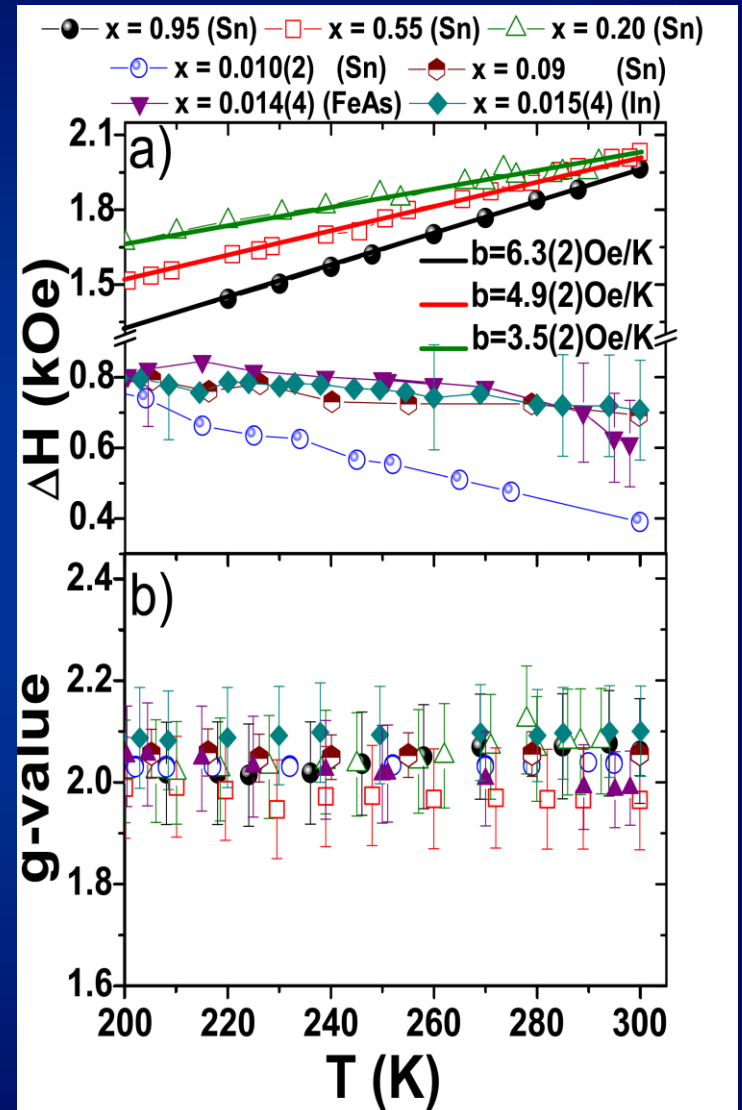
Results – ESR – $\text{Ba}_{1-x}\text{Eu}_x\text{Fe}_2\text{As}_2$

- Decreasing Korringa rate.
- T and x independent g-factor.



$$\Delta g = J_{fs}(0) \frac{\eta(E_F)}{1 - \alpha}$$

$$\frac{d(\Delta H)}{dT} = \frac{\pi k}{g\mu_B} \langle J_{fs}^2(\mathbf{q}) \rangle \eta^2(E_F) \frac{K(\alpha)}{(1 - \alpha)^2}$$



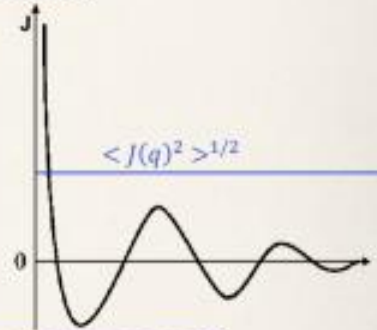
ESR Results

q-dependence of the exchange interaction

$$b_{\text{calculated}} > b_{\text{measured}}$$

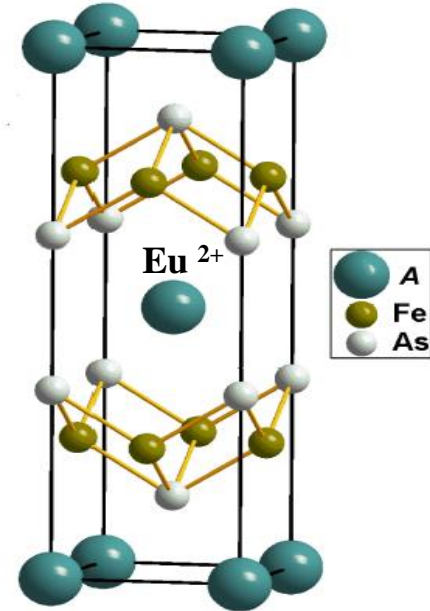
$$\Delta g = J_{fs}(\mathbf{0}) \frac{N(E_F)}{1 - \alpha} \quad \text{Stoner enhancement factor}$$

$$\frac{d(\Delta H)}{dT} = \frac{\pi k}{g\mu_B} \langle J_{fs}^2(\mathbf{q}) \rangle N(E_F)^2 \frac{K(\alpha)}{(1 - \alpha)^2}$$

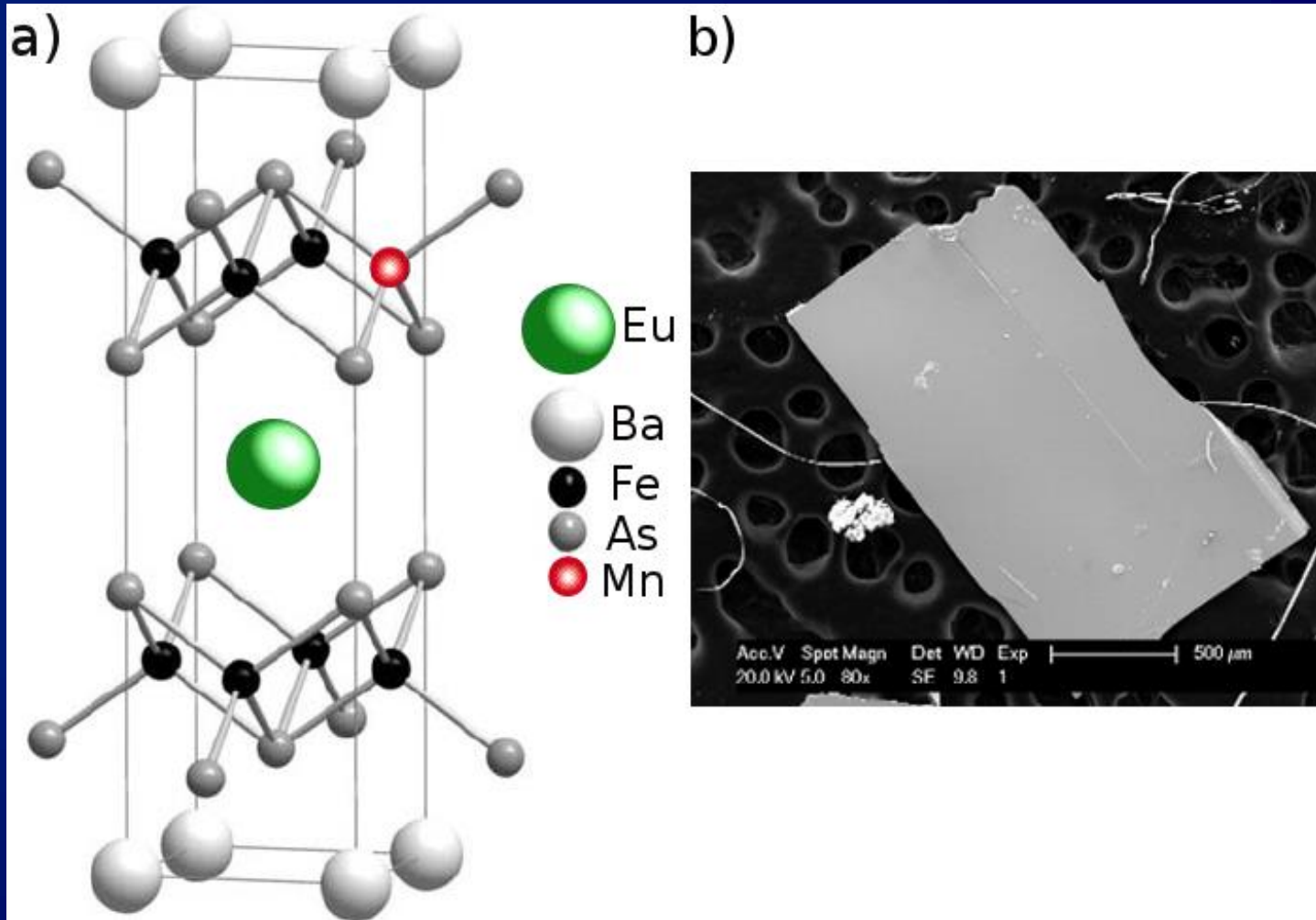


Decreasing Korringa rate (b) \longrightarrow Decreasing $\langle J_{fs}(\mathbf{q}) \rangle$

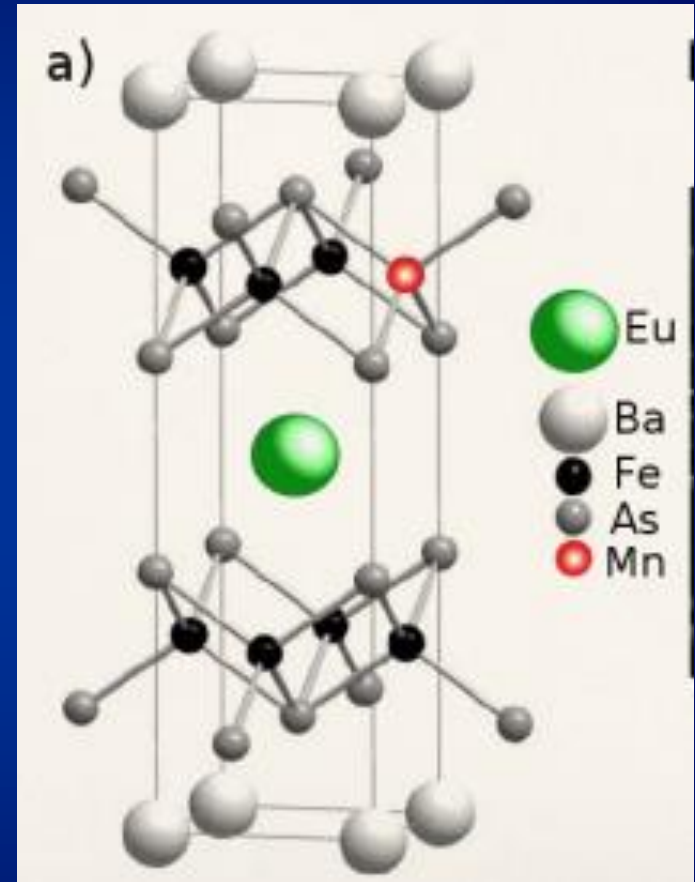
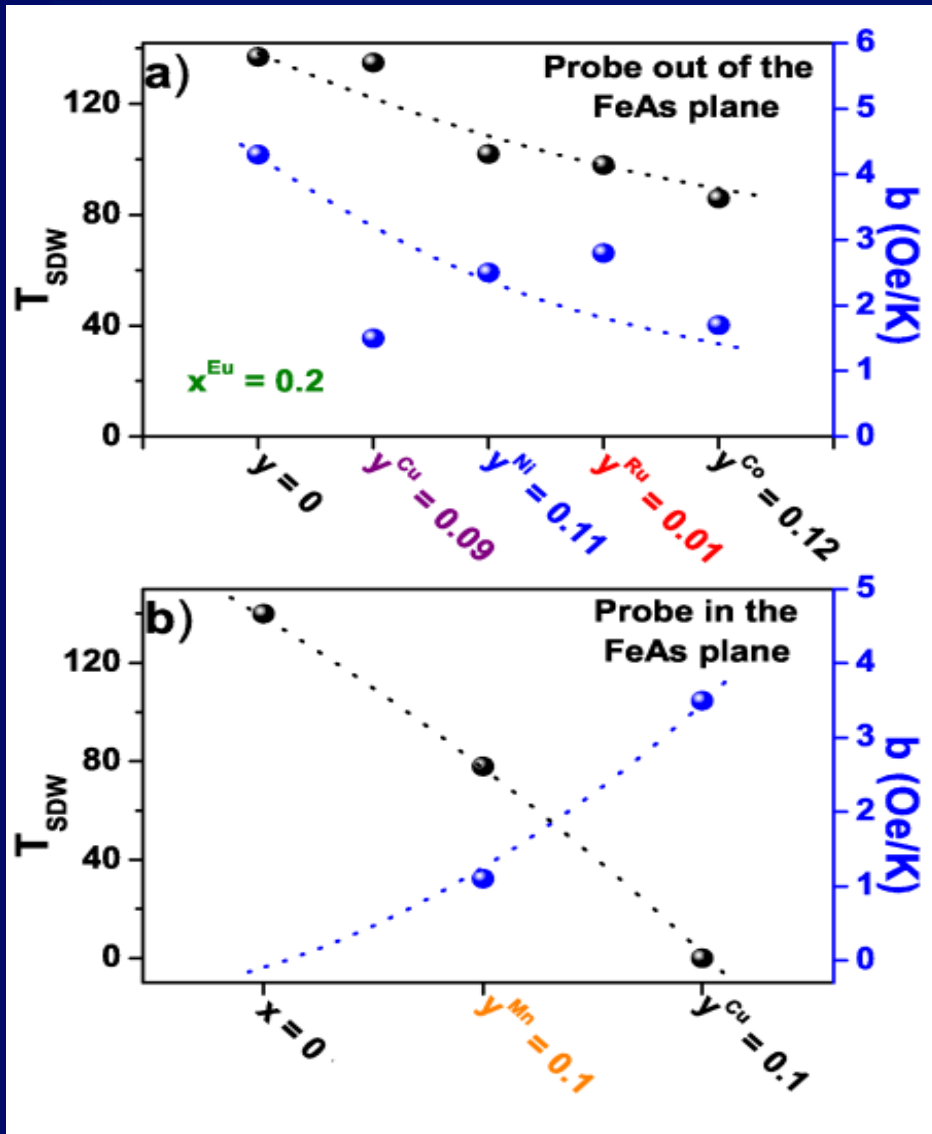
- 3d Fe bands are becoming more anisotropic
- • (less s-like) and are, in average, further away from the Eu sites.



Site specific ESR on Fe-based Intermetallic Compounds

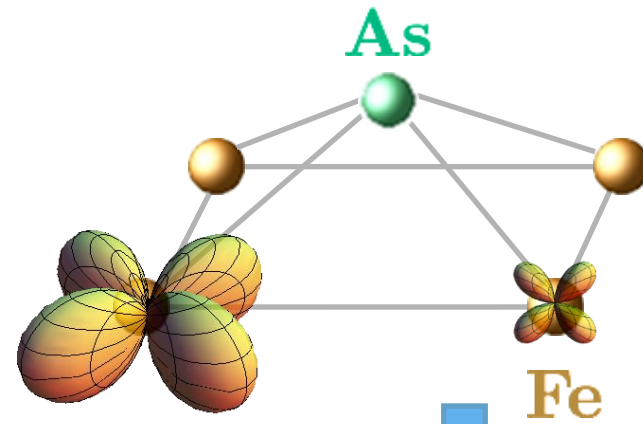
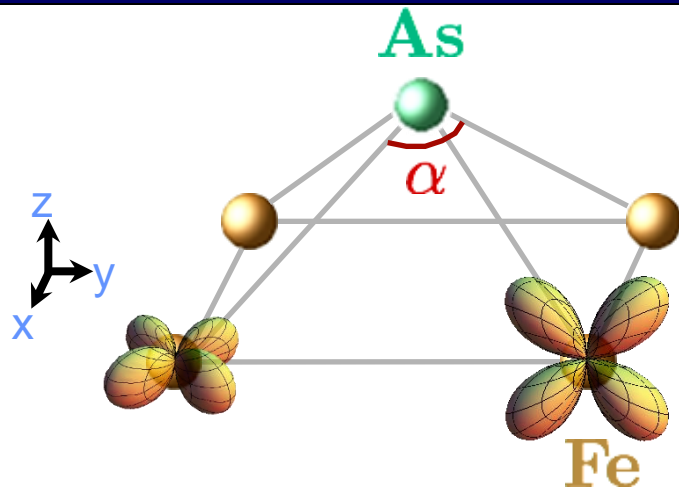


ESR – Results – Site Specific



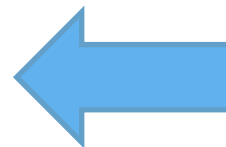
P. F. S. Rosa...PG. Pagliuso et al. PHYSICAL REVIEW B **86**, 165131 (2012)

P. F. S. Rosa...PG Pagliuso et al. Nature-Scientific Reports **4**, 6543 (2014) *ibid* Nature-Scientific Reports **4**, 6252 (2014)



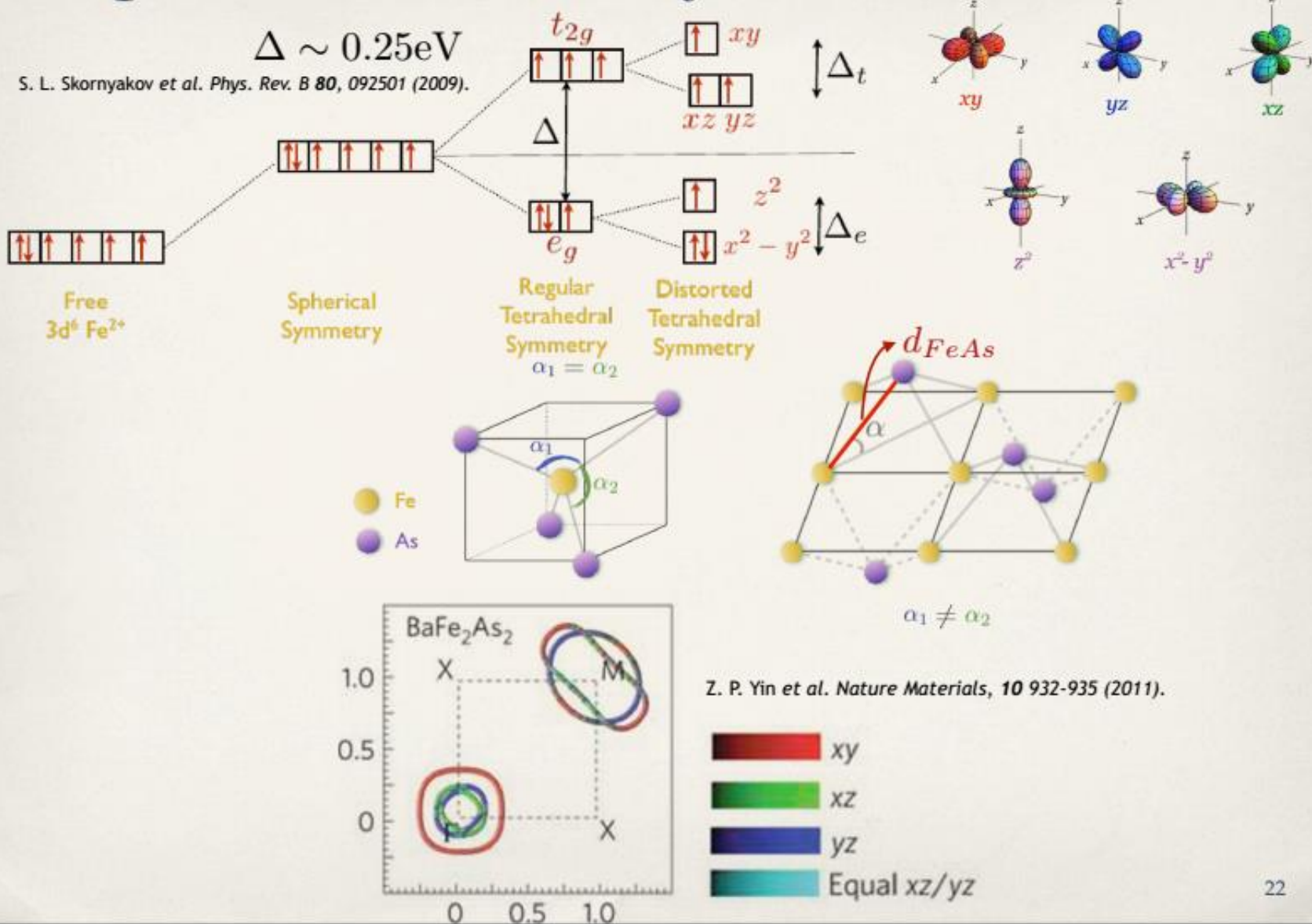
Smaller $d_{\text{Fe-As}}$ with
chemical substitution,
hydrostatic pressure
and magnetic field in
the plane!

SDW Phase vanishes



xy occupation increases

Importance of the Crystal Field



Quantum Oscillations Results

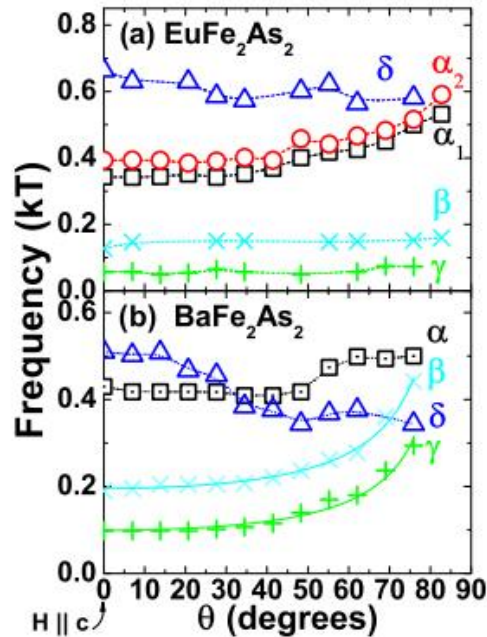
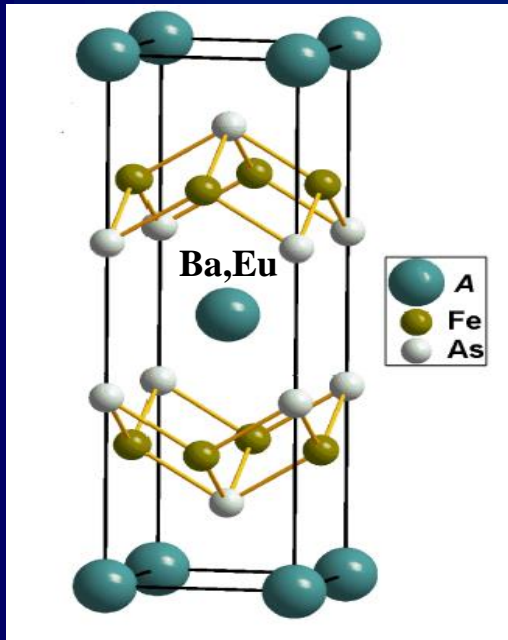


FIG. 4. (Color online) Angular field dependence (anisotropy) of the observed QO frequencies of (a) EuFe_2As_2 (Eu122) and (b) BaFe_2As_2 (Ba122).

The calculated effective masses m_{DFT}^* also display agreement with the experimental data, as shown in Table I. We note that an ideal quantitative agreement of effective masses is often

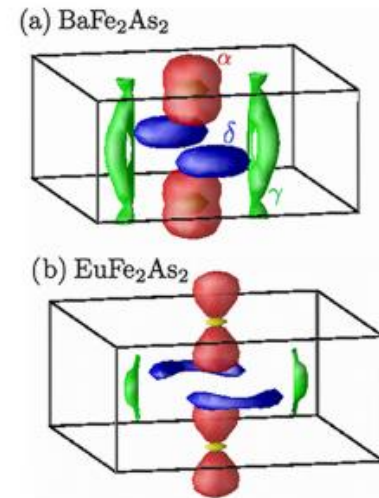


FIG. 5. (Color online) The shifted Fermi surfaces of (a) BaFe_2As_2 and (b) EuFe_2As_2 compounds in the magnetic phase. We identify the large hole sheet (red) as the α pocket, the crescent electron sheet (blue) as the δ pocket, and the tubelike electron pocket (green) as the γ pocket.

195146-4

- Eu122 displays a much more isotropic and three-dimensional-like FS when compared with Ba122.
- Results suggest an anisotropic contribution of the Fe 3d orbitals to the FS in Ba122. We speculate that this orbital differentiation may be responsible for the suppression of the SDW phase in the FeAs-based compounds.

Combined external pressure and chemical substitution results

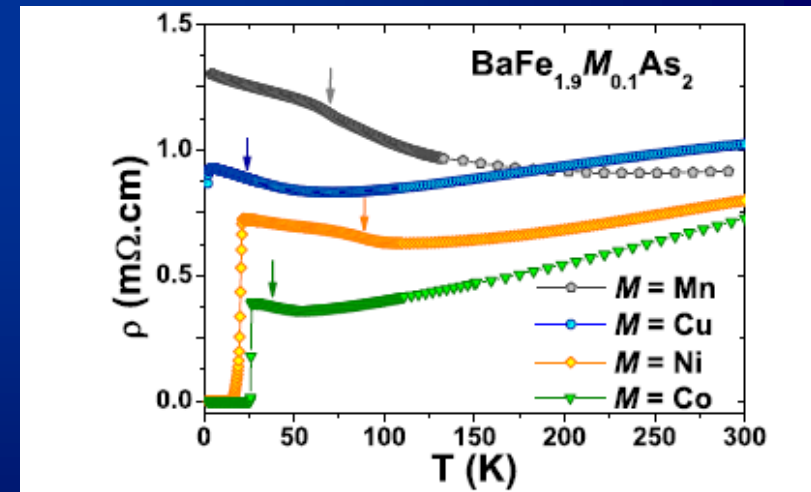
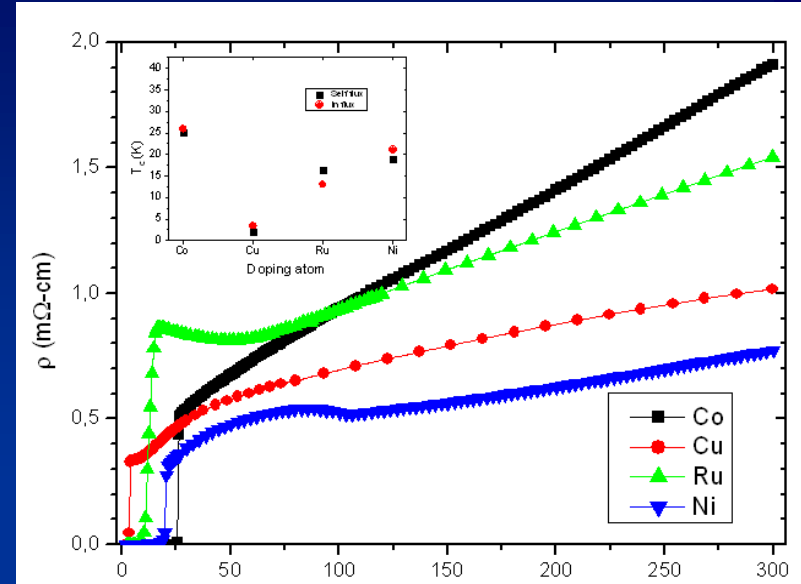
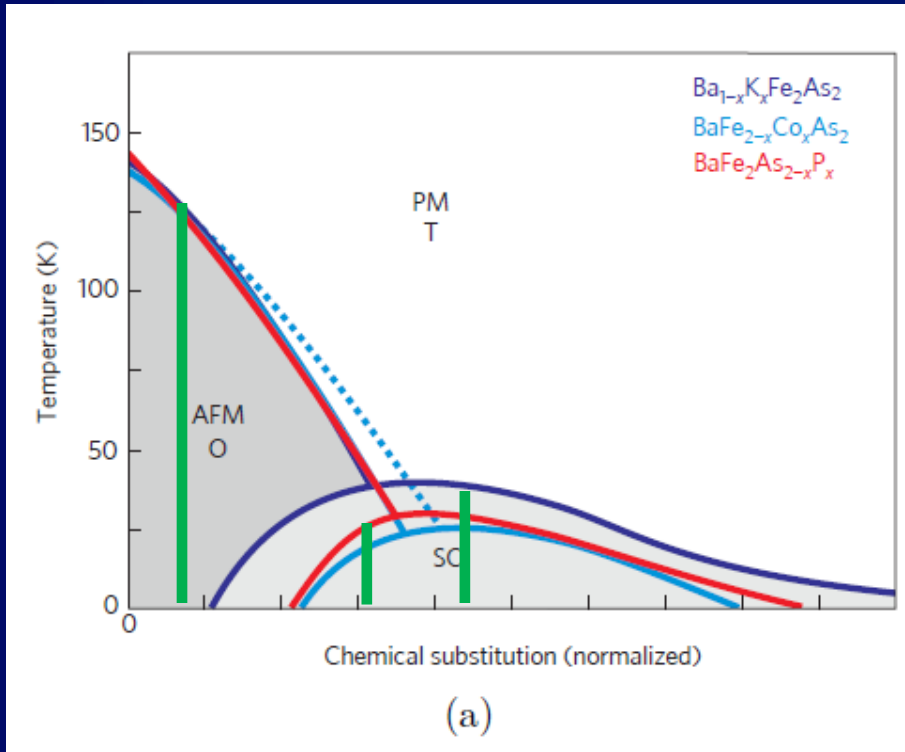


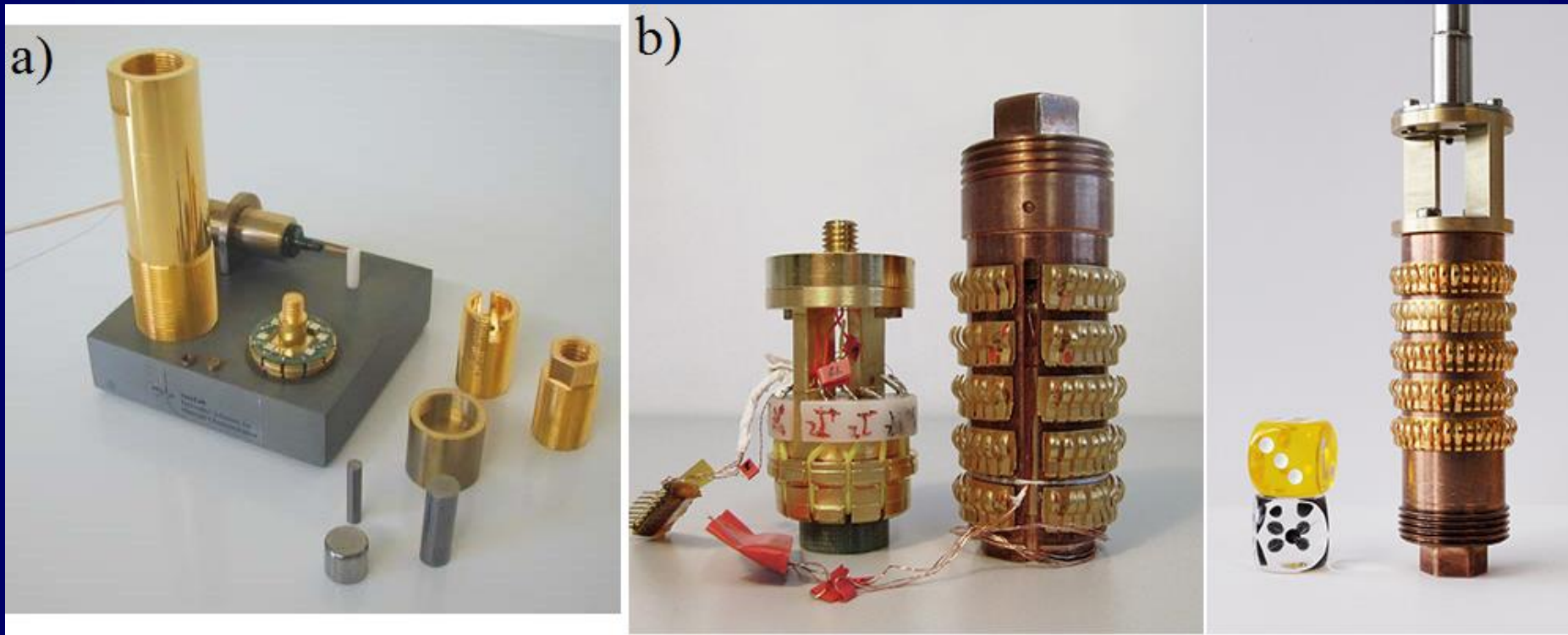
Figure 1 | In-plane electrical resistivity, $\rho_{ab}(T)$, for $BaFe_{1.9}M_{0.1}As_2$ ($M = Mn, Cu, Ni, Co$) single crystals. The arrows show the minima of the first derivative in the vicinity of the SDW transition.

- Different P-dependences are expected as a function of x for substituted samples!

Combined external pressure and chemical substitution results

Experimental Details

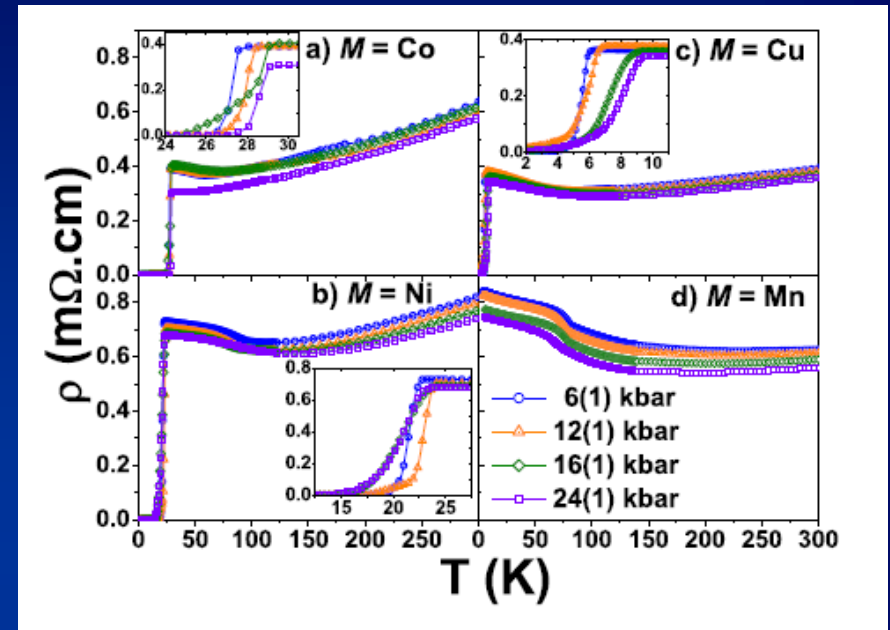
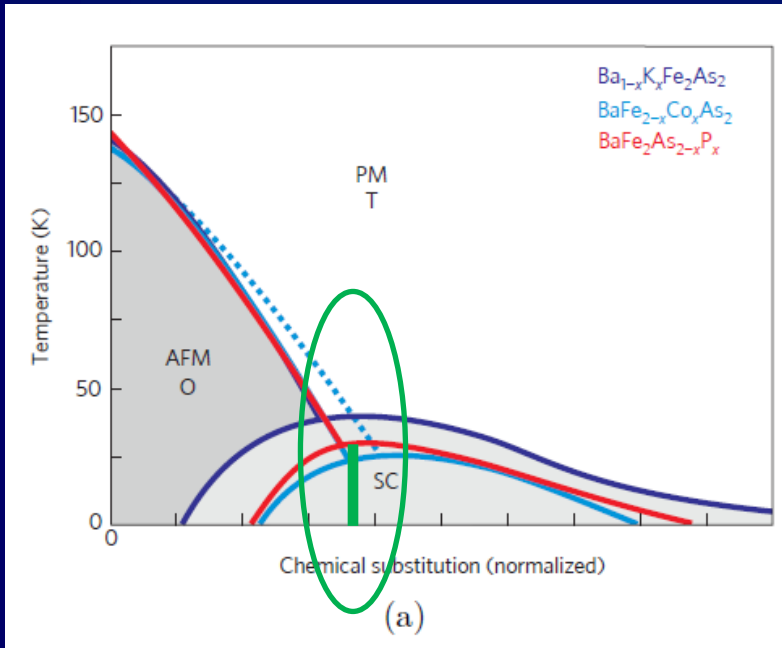
- In-plane electrical resistivity under quasi-hydrostatic pressure:



Extracted from Application Note on Pcell 15/30

Extracted from <<http://www.dilatometer.info/>>

Combined external pressure and chemical substitution results



- Very weak (increasing) T_c -dependence as a function of P for $M = Co$ or Ni for x near OPD region, as expected.
- Surprisingly, T_c increases more than a factor of two as a function of pressure for $M = Cu$.

Combined external pressure and chemical substitution results

- Abrikosov-Gokov - IMPB

$$\left| \frac{\Delta T_c}{\Delta c} \right| = \frac{\pi^2}{8} \eta(E_F) \langle J^2(\mathbf{q}) \rangle S(S+1),$$

- ESR Korringa rate.

$$\frac{d(\Delta H)}{dT} = \frac{\pi k}{g\mu_B} \langle J_{fs}^2(\mathbf{q}) \rangle \eta^2(E_F)$$

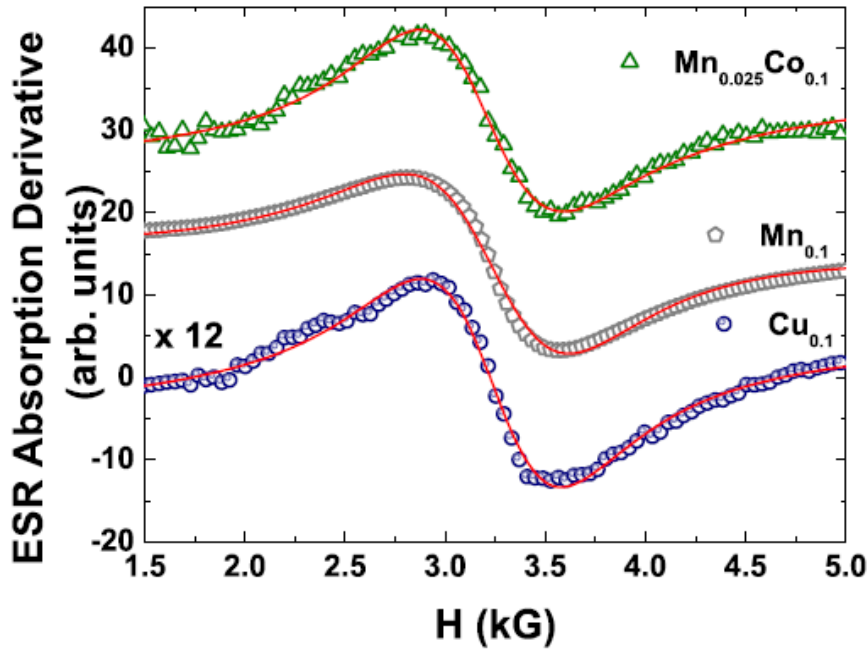
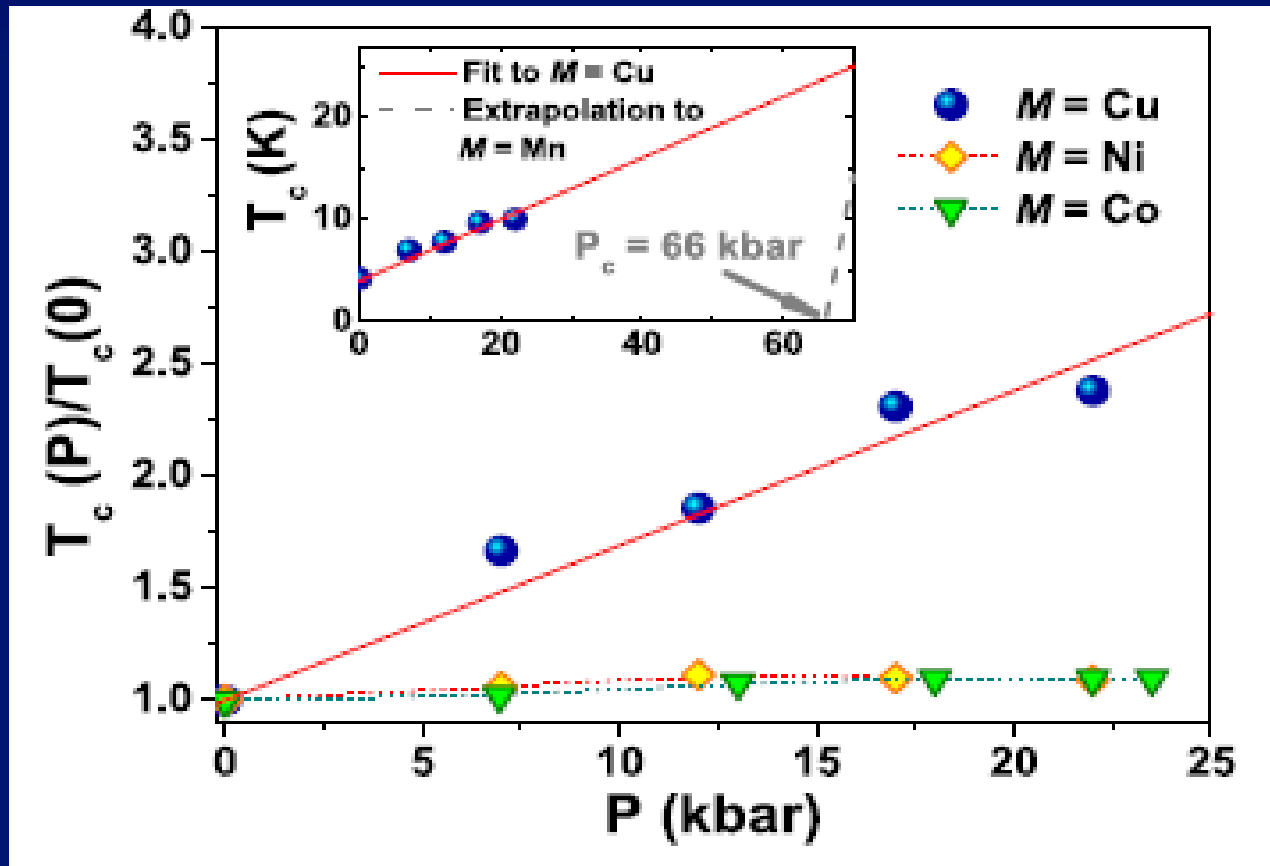


Table I | Experimental and calculated parameters for BaFe_{1-x}M_yAs₂ (this work) and conventional SC (refs. [31, 37])

Sample	c (%)	g _{ESR}	\Delta T _c ^{exp} (K)	T _{c,0} (K)	\langle J ² (q) \rangle _{ESR}^{1/2} (meV)}	\langle J ² (q) \rangle _{AG}^{1/2} (meV)}
BaFe _{1.9} Cu _{0.1} As ₂	5	2.08(3)	22	26	1.2(5)	111(10)
BaFe _{1.88} Mn _{0.12} As ₂	6	2.05(2)	≥ 26	26	0.7(5)	≥ 32(3)
BaFe _{1.895} Co _{0.100} Mn _{0.005} As ₂	0.25	2.06(2)	10	26	0.8(5)	98(9)
Lu _{1-x} Gd _x Ni ₂ B ₂ C	0.5	2.035(7)	≈ 0.3	15.9	10(4)	11(1)
Y _{1-x} Gd _x Ni ₂ B ₂ C	2.1	2.03(3)	≈ 0.9	14.6	9(3)	10(1)
La _{1-x} Gd _x Sn ₃	0.4	2.010(10)	≈ 0.5	6.4	20(2)	≈ 20(2)

Combined external pressure and chemical substitution results

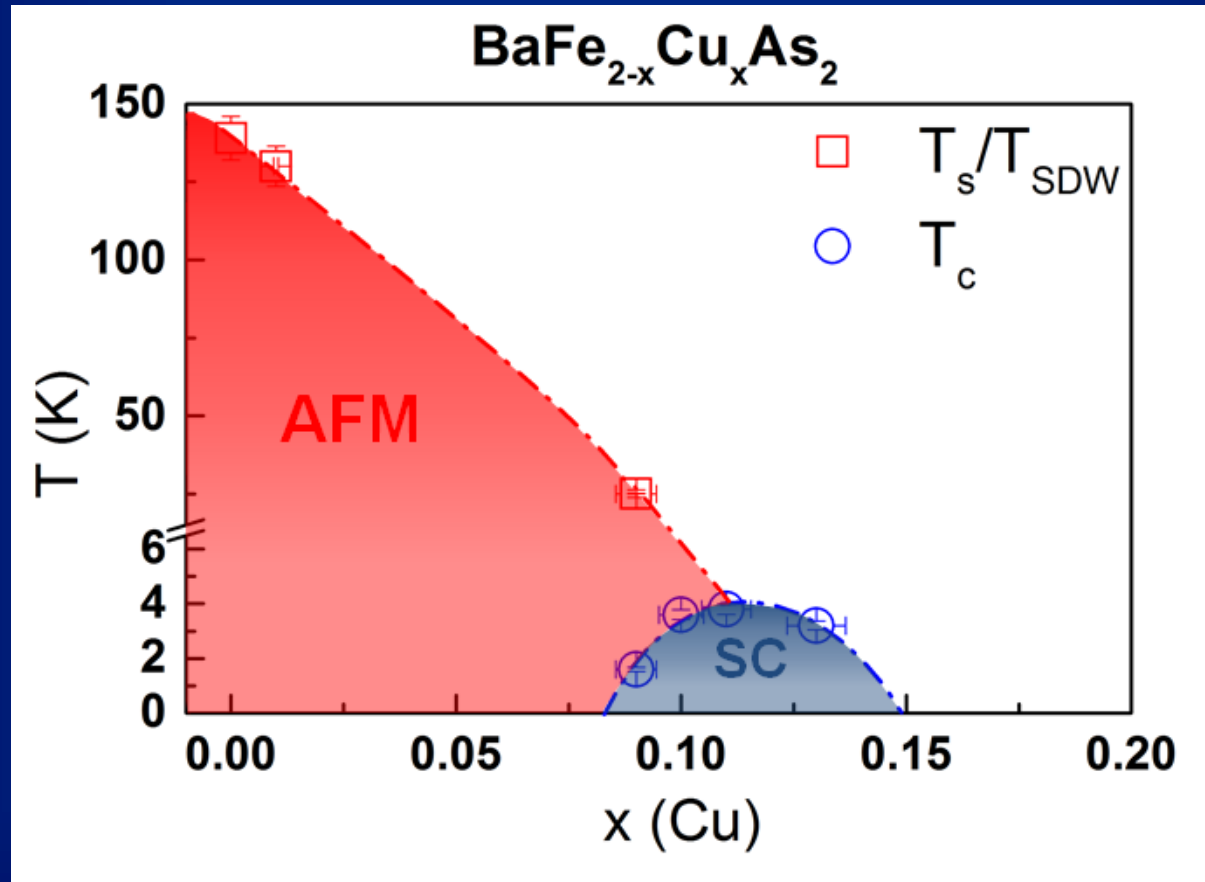


the SC domes. The linear fit for the $M = \text{Cu}$ compound (solid line) was obtained from the phenomenological expression $\Delta T_c = S(S + 1)(a - bP)$. Using the same expression and $S = 5/2$, we obtain the dashed line for the $M = \text{Mn}$ compound.

- BaCu_2As_2 is a Pauli metal!

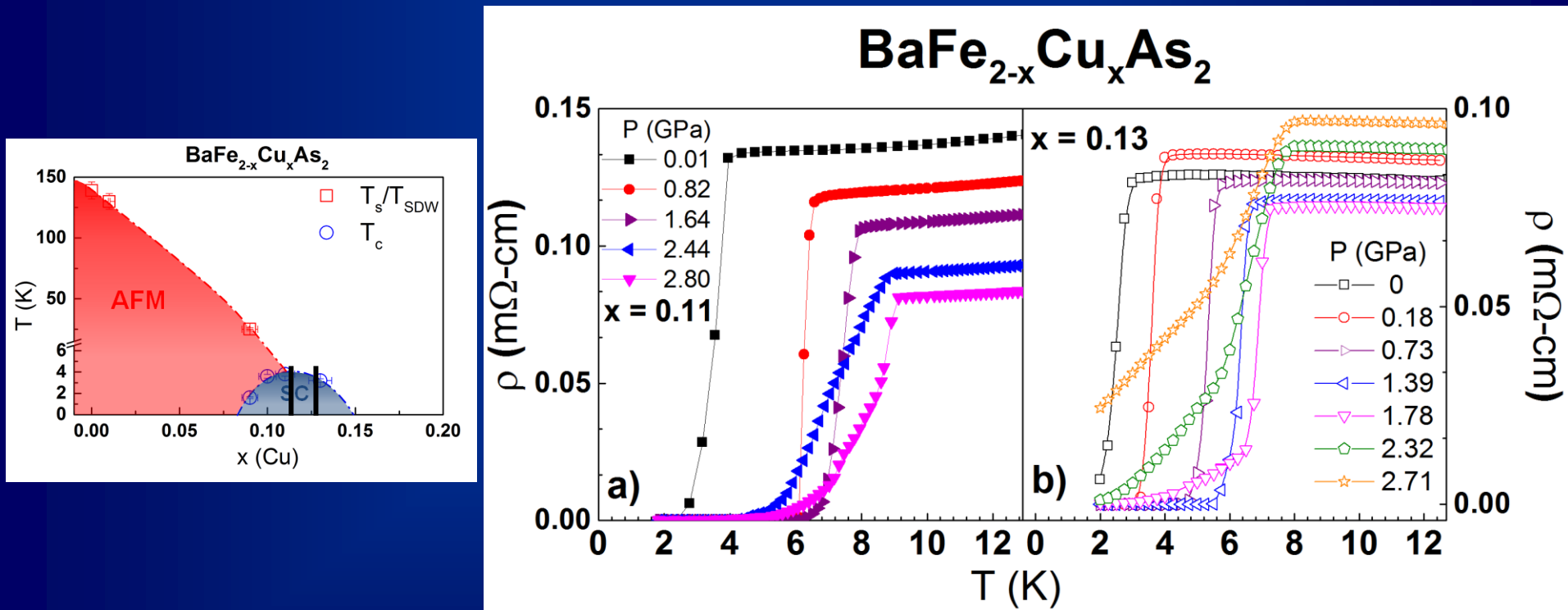
Combined external pressure and chemical substitution results

- Temperature-composition phase diagram:



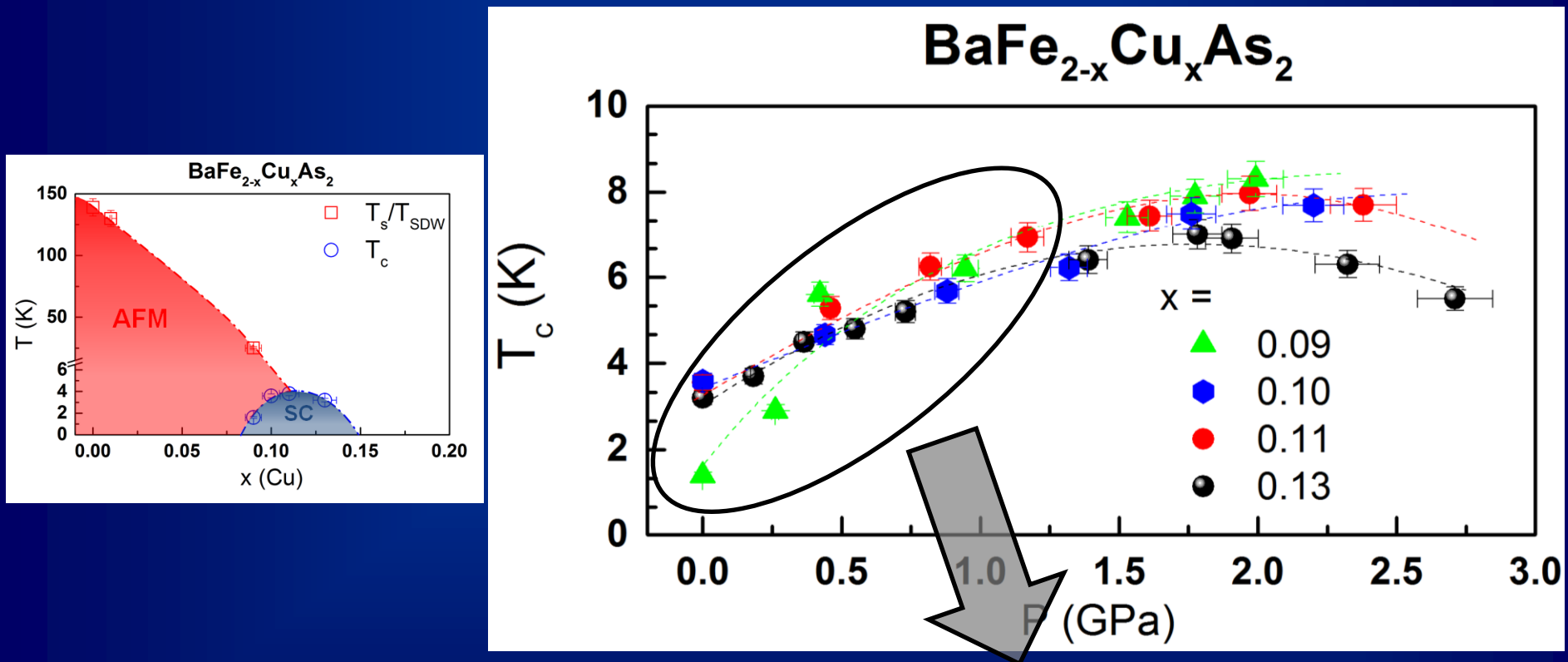
Combined external pressure and chemical substitution results

- In-plane electrical resistivity at several pressures around the ODP limit:



Combined external pressure and chemical substitution results

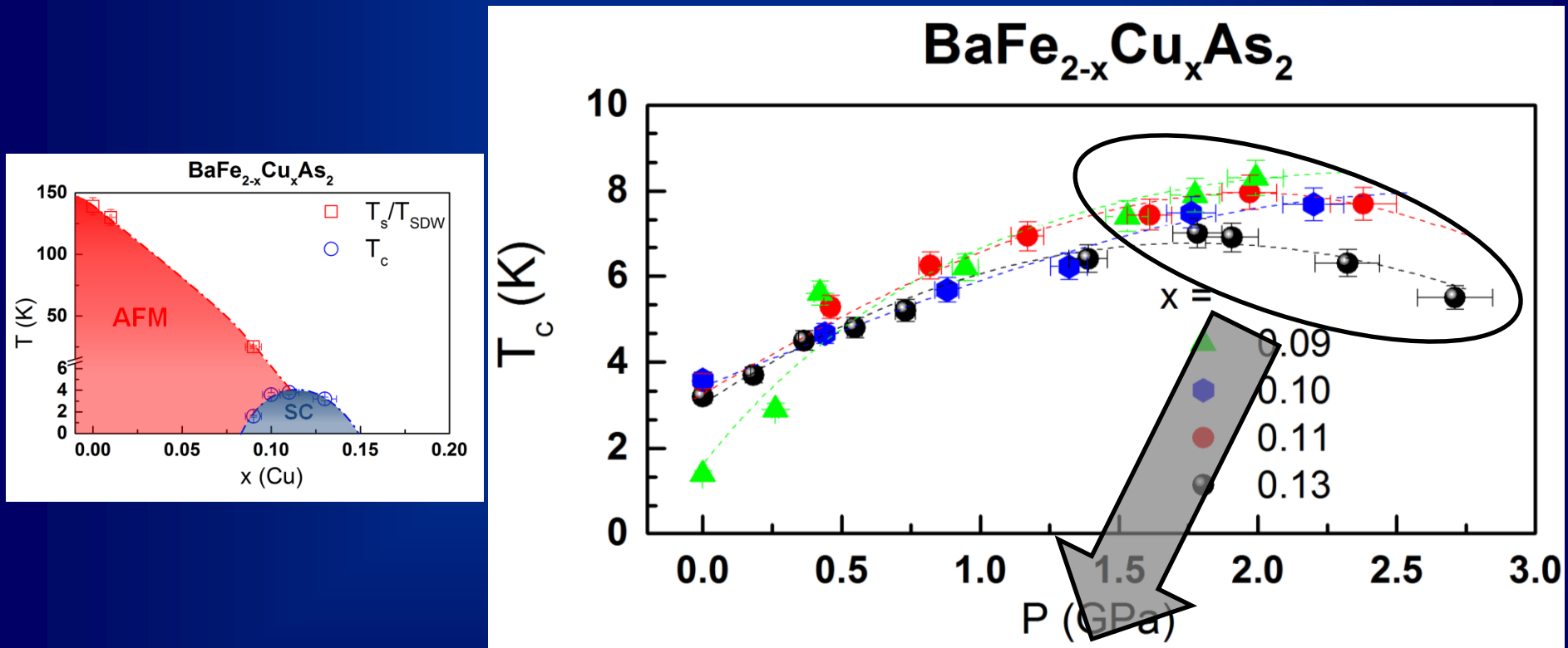
- Temperature-pressure phase diagram for Cu concentrations around the SC OPD:



Increase of T_c as a function of pressure

Combined external pressure and chemical substitution results

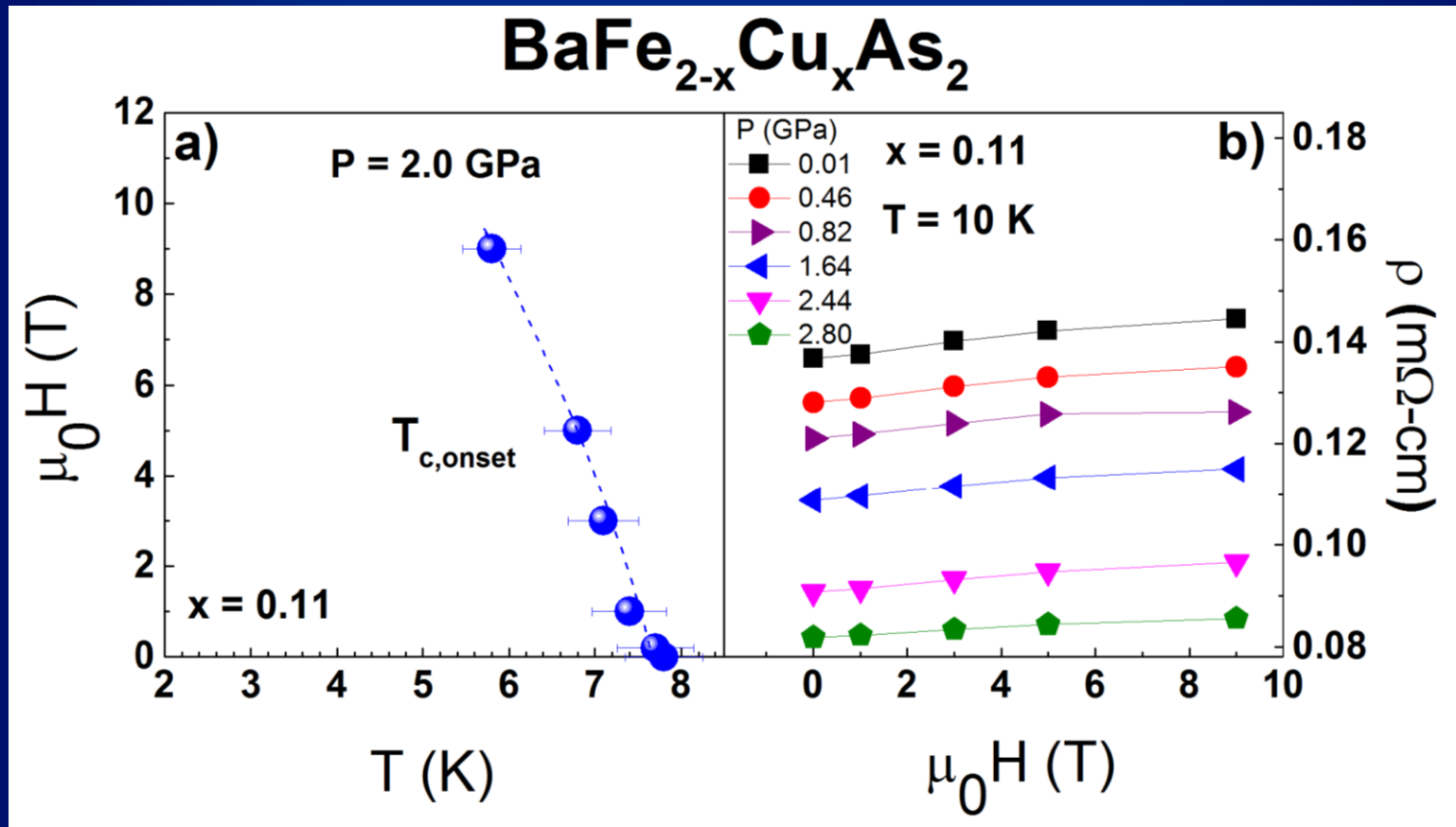
- Temperature-pressure phase diagram for almost all the Cu concentrations of the SC dome:



Tendency to saturation and decreasing of T_c

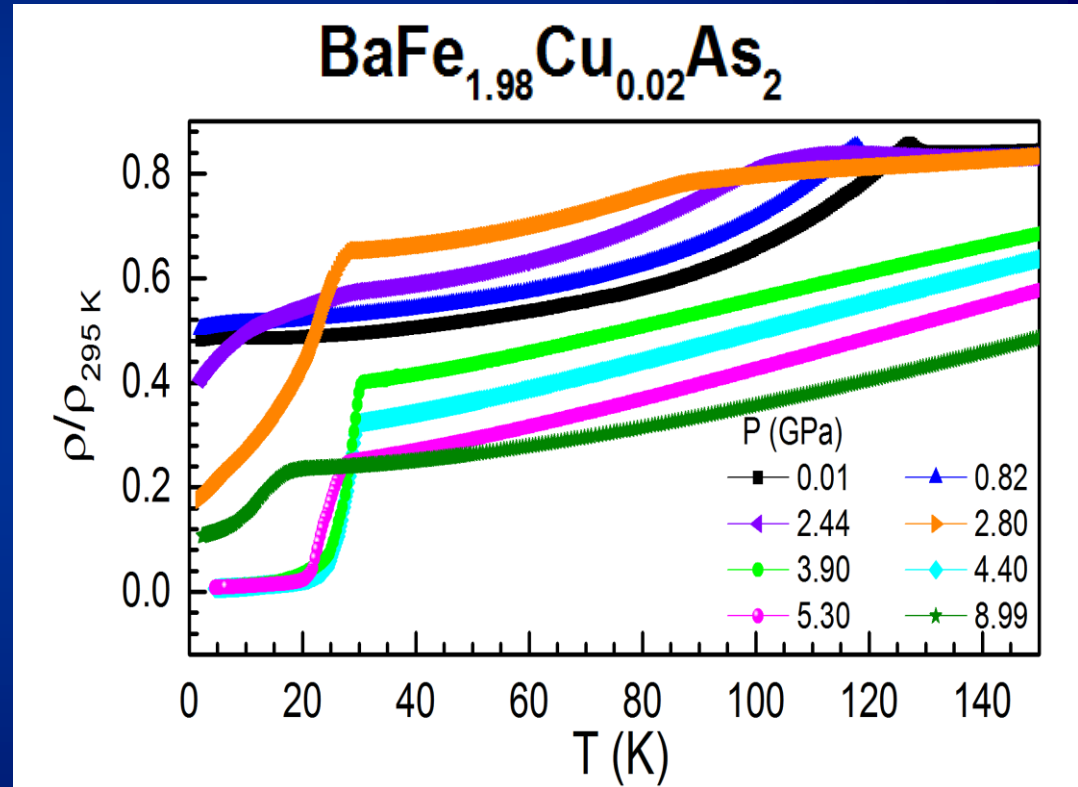
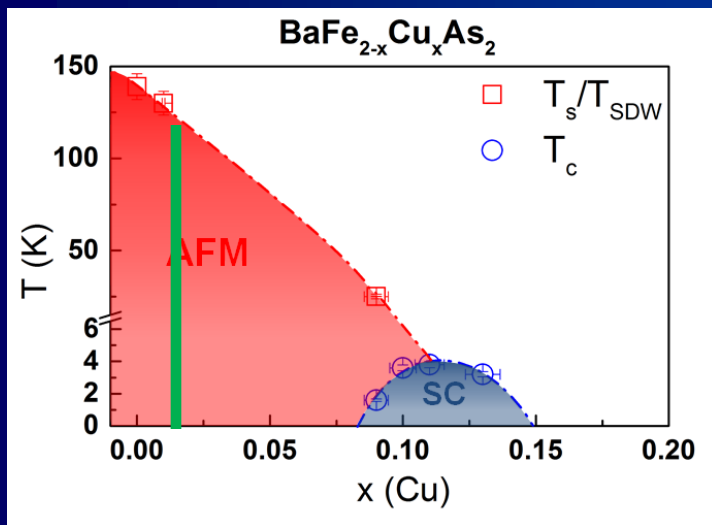
Combined external pressure and chemical substitution results

- Magnetic field dependence of T_c and magneto resistance for the OPD compound at several pressures:



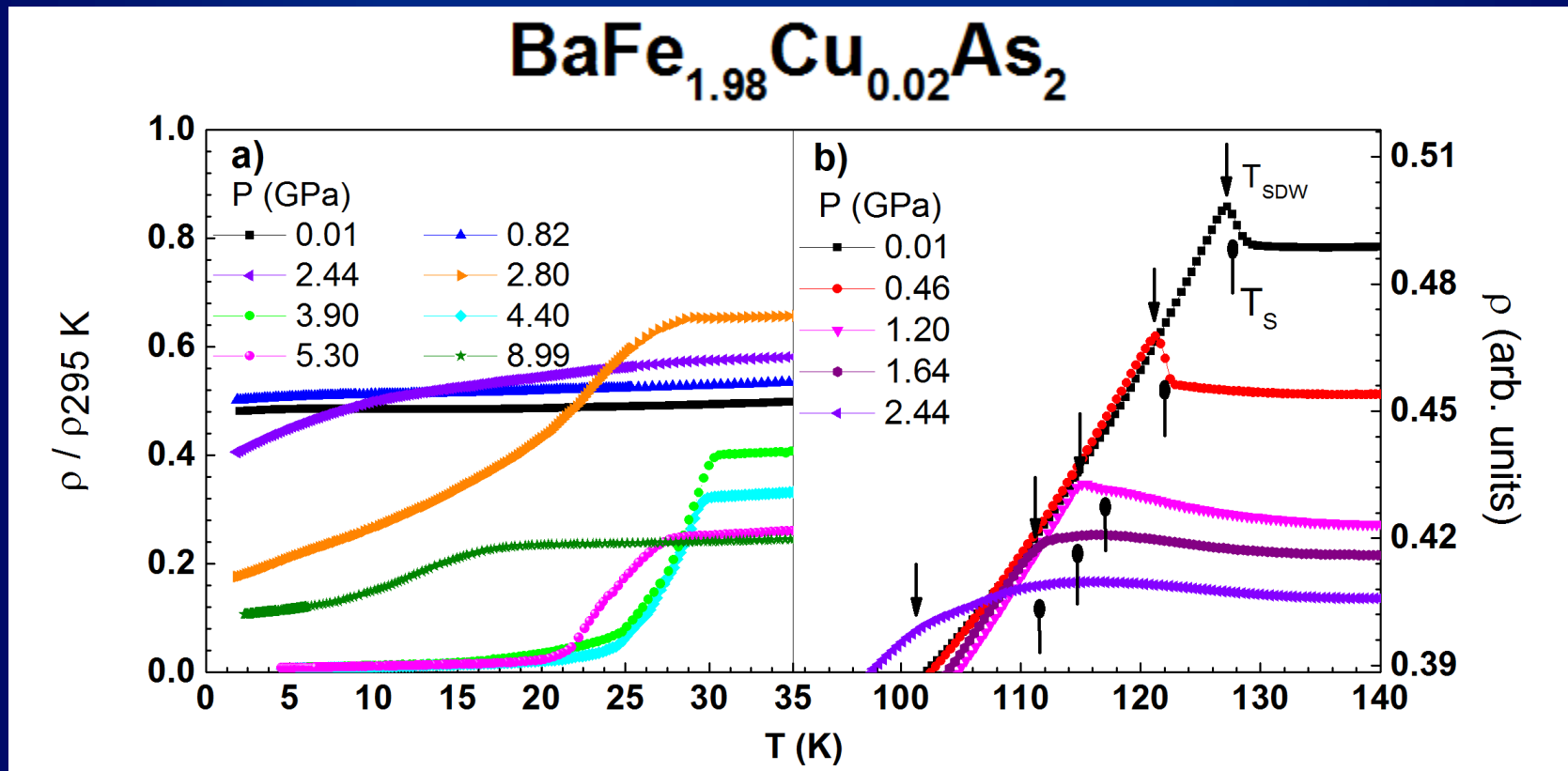
Combined external pressure and chemical substitution results

- In-plane electrical resistivity for the under doped compound at several pressures:



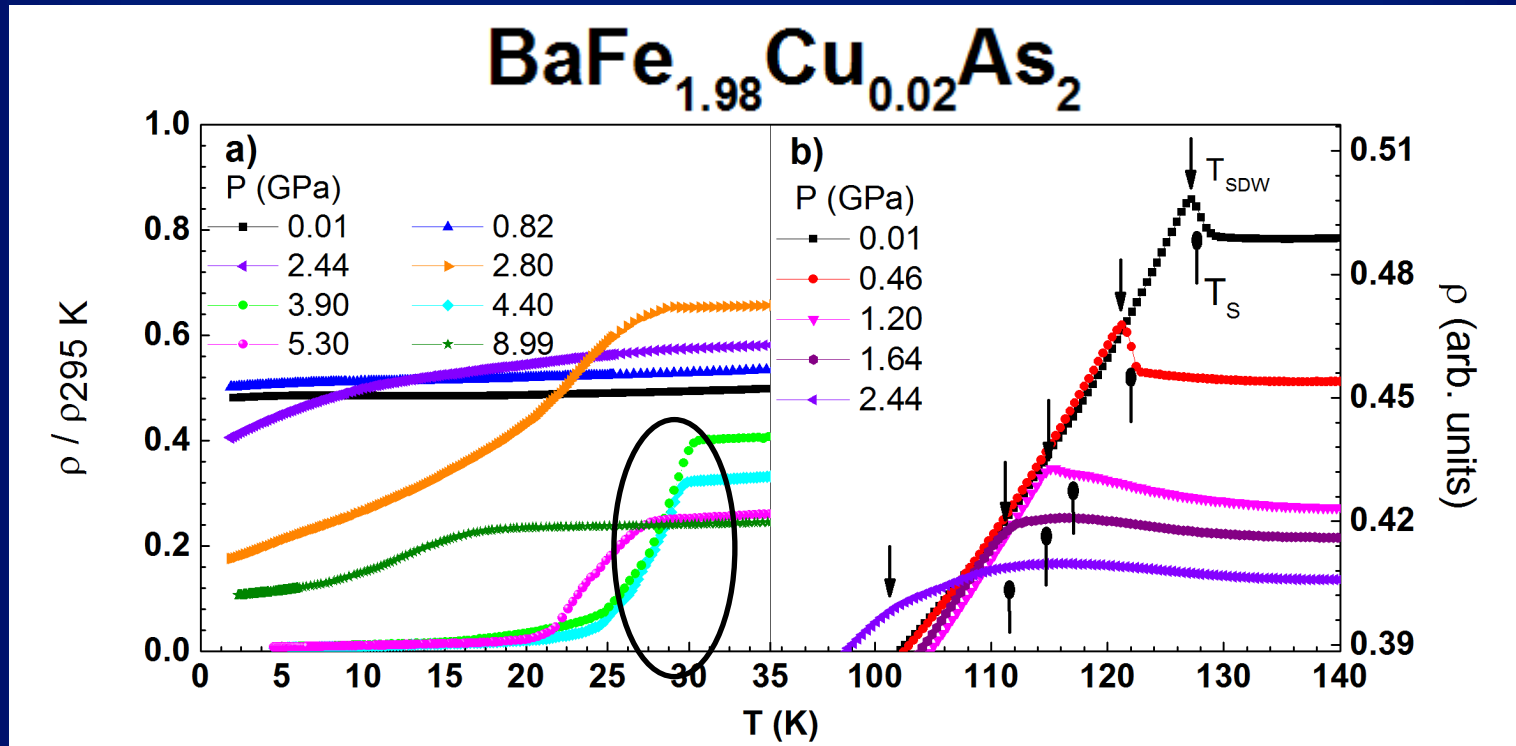
Combined external pressure and chemical substitution results

- Zoom in the transition temperatures:



Combined external pressure and chemical substitution results

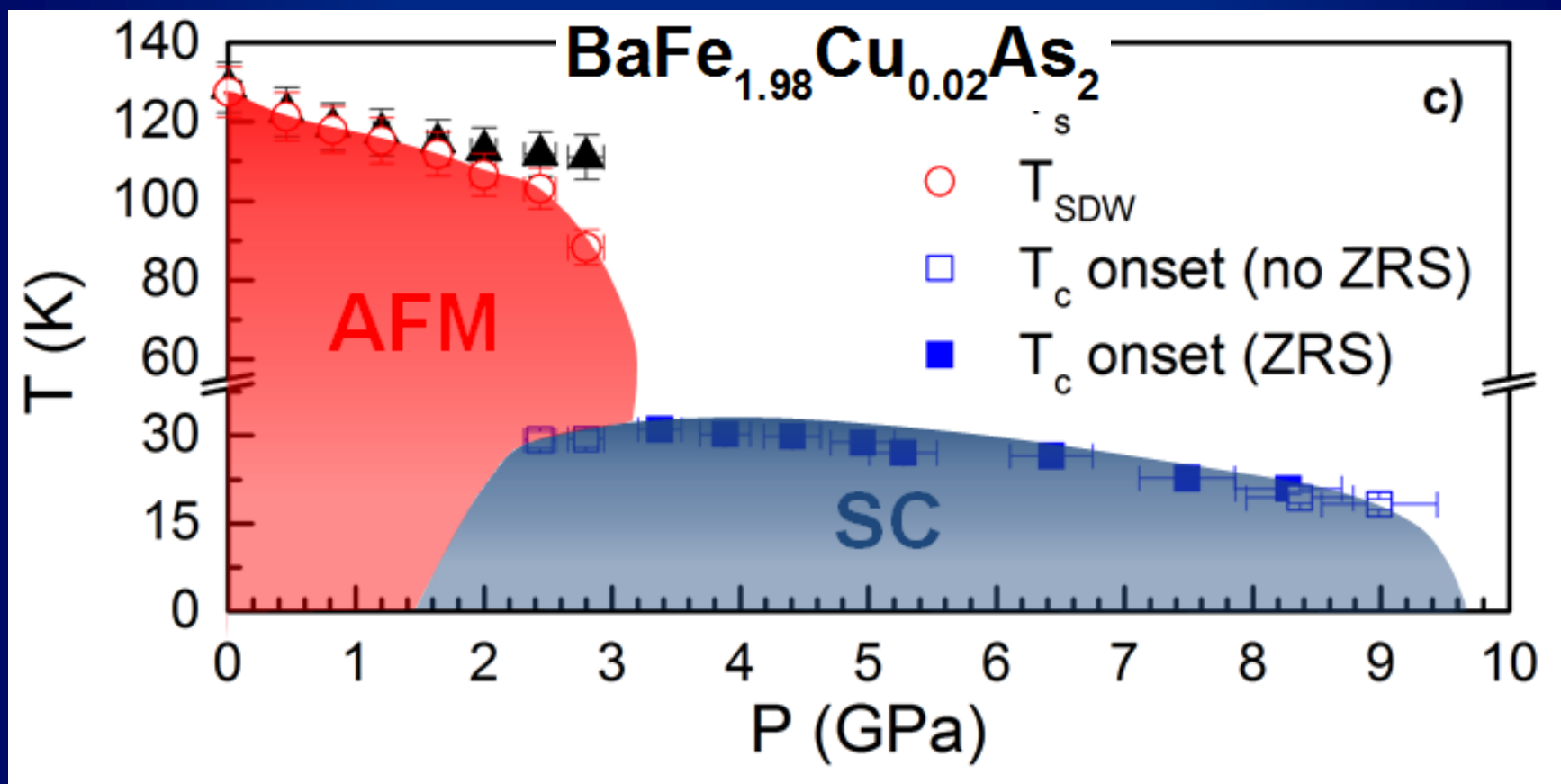
- Zoom in the transition temperatures:



This value of T_c is close to the maximum T_c achieved in the pure compound under pressure

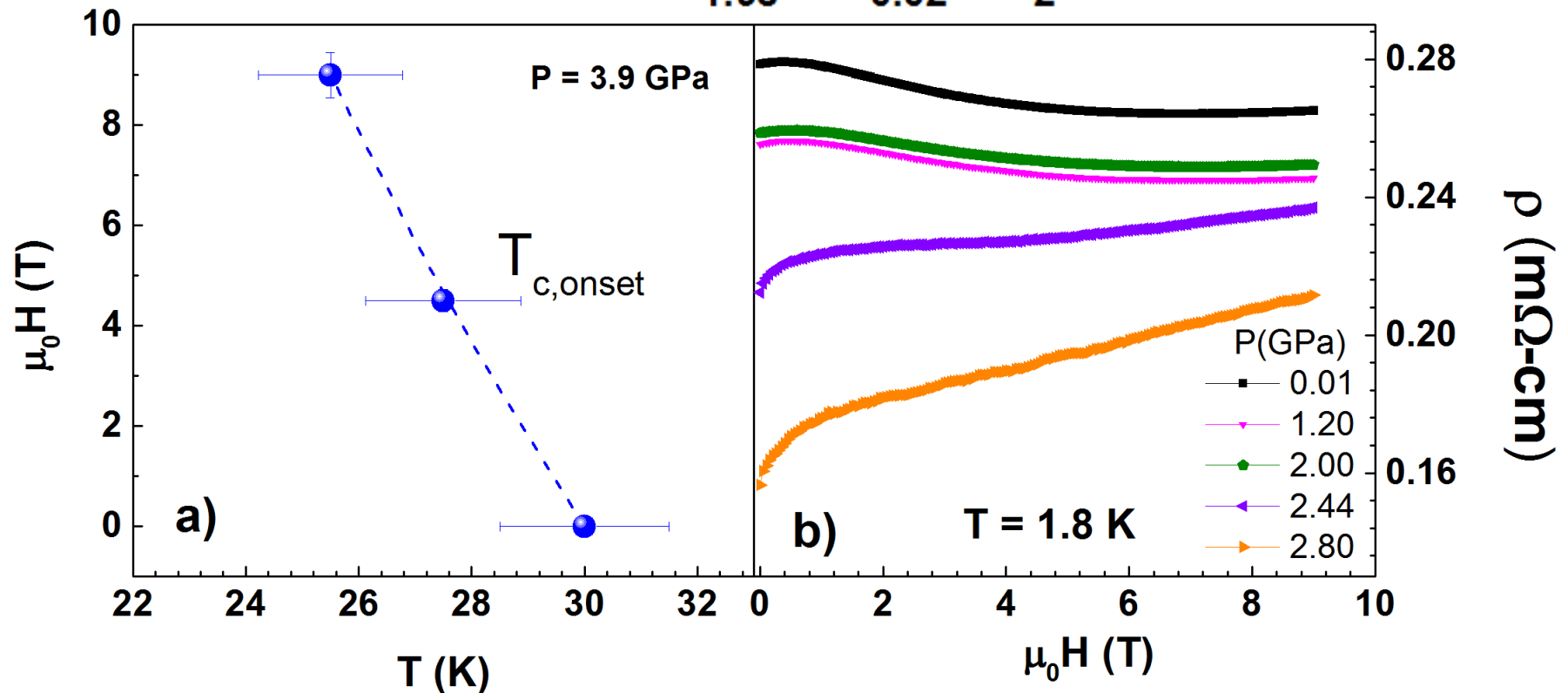
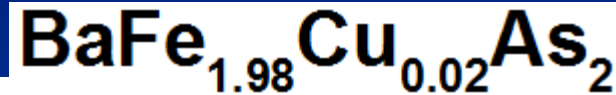
Combined external pressure and chemical substitution results

- Temperature-pressure phase diagram for the under doped sample:

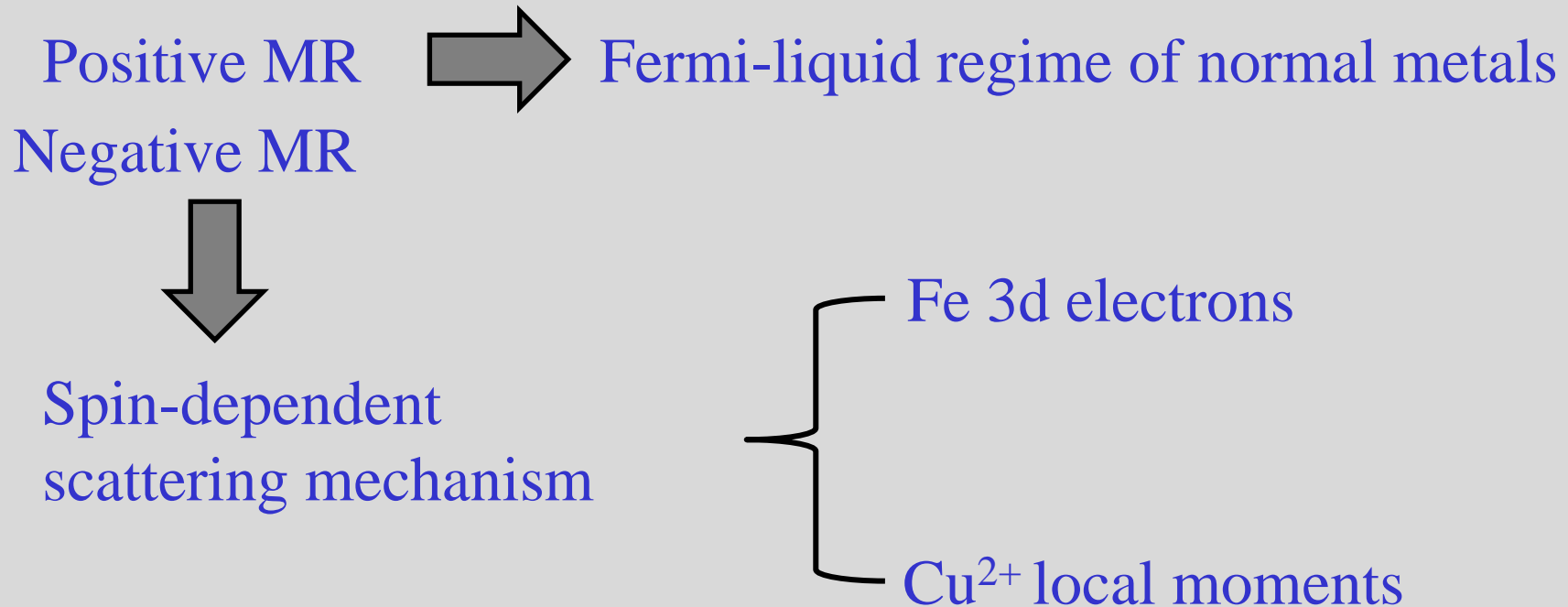


Combined external pressure and chemical substitution results

- Magnetic field dependence of T_c and magneto resistance for the under doped compound at several pressures:



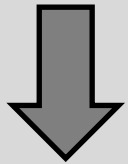
Combined external pressure and chemical substitution results



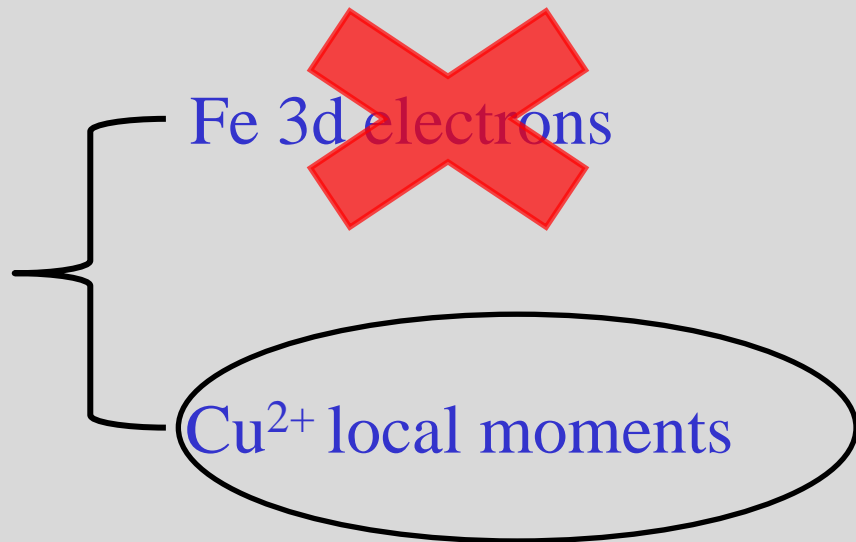
Combined external pressure and chemical substitution results

Positive MR → Fermi-liquid regime of normal metals

Negative MR



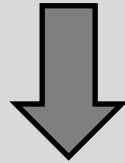
Spin-dependent scattering mechanism



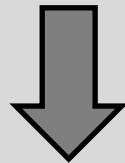
Impurity magnetic pair-breaking effect

Combined external pressure and chemical substitution results

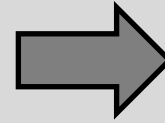
Impurity magnetic
pair-breaking effect



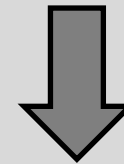
Cu-substitution
(BaCu₂As₂ is a
Pauli paramagnet)



Consistent with the
positive MR in OPD
samples



Applied
pressure



Screening of Cu²⁺
local moments



Great enhancement
of T_c

Final Remarks

- Fe 3d bands orbital differentiation induced by local distortions of the dFe-As seem to be most relevant tuning parameter to drive the SDW phase to SC in Ba112.
- Cu^{2+} and Mn^{2+} spins give rise to a non-conventional IPB mechanism in substituted Ba112 system
- Cu-substituted Ba112 show screening/suppression of the Cu^{2+} spins as a function of pressure and Cu-concentration.
- Low-x Cu substitution samples show the same pressure induced T_c around 30 K as the pure compound.
- Evolution of a negative MR to a positive one as a function of pressure or Cu substitution.

Acknowledgments



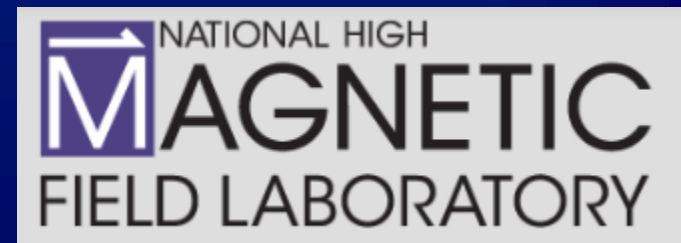
Collaboration



UC - Irvine



CBPF



GPOMS - “FeAs” Team



Prof. Dr. Ricardo Urbano
(urbano@ifi.unicamp.br)



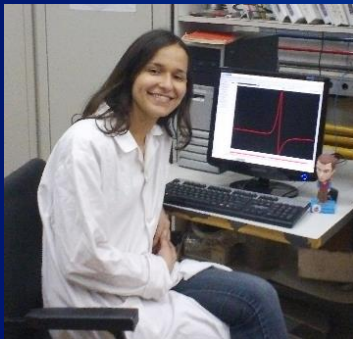
Prof. Dr. Eduardo Granado
(egranado@ifi.unicamp.br)



Prof. Dra Cris Adriano
(cadriano@ifi.unicamp.br)



Dr. Eduardo Bittar



Dra. Priscila Rosa



Dr. Thales Garitezi

“FeAs” Team – Next Generation



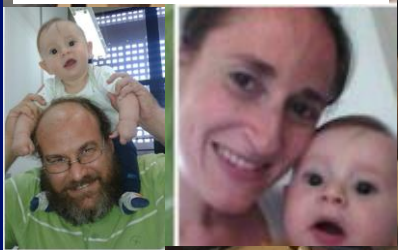
Matheus Radaelli

Mario Piva

Camilo B. de Jesus

Guilherme Lesseux

Martin/Dina e Nicolás





That's all folks!

Thank you for your attention!